Consequences of a telomerase-related fitness defect and chromosome substitution technology in yeast synIX strains

Laura Mcculloch, Vijayan Sambasivam, Amanda Hughes, Narayana Annaluru, Sivaprakash Ramalingam, Viola Fanfani, Evgenii Lobzaev, Leslie Mitchell, Jitong Cai, Hua Jiang, et al.

Consequences of a telomerase-related fitness defect and chromosome substitution technology in yeast *synIX* strains

Laura H. McCulloch, [1,22] Vijayan Sambasivam, [2,22] Amanda L. Hughes, [3] Narayana Annaluru, [2,17] Sivaprakash Ramalingam, [2,21] Viola Fanfani, [4,19] Evgenii Lobzaev, [4,5] Leslie A. Mitchell, [1,20] Jitong Cai, [6] The Build-A-Genome Class [6,7,8] Hua Jiang, [9] John LaCava, [9,10] Martin S. Taylor,[11] William R. Bishai,[12] Giovanni Stracquadanio,[4] Lars M. Steinmetz,[3,14,15] Joel S. Bader,[6,13] Weimin Zhang, [1,*] Jef D. Boeke, [1,13,16,23,*] and Srinivasan Chandrasegaran [2,18,*]

The Build-A-Genome Class authors: Breeana G. Anderson, Abena Apaw, Pavlo Bohutskyi, Erin Buchanan, Daniel Chang, Melinda Chen, Eric Cooper, Amanda Deliere, Kallie Drakos, Justin Dubin, Christopher Fernandez, Zheyuan Guo, Thomas Harrelson, Dongwon Lee, Jessica McDade, Scott Melamed, Héloise Muller, Adithya Murali, José U. Niño Rivera, Mira Patel, Mary Rodley, Jenna Schwarz, Nirav Shelat, Josh S. Sims, Barrett Steinberg, James Steinhardt, Rishi K. Trivedi, Christopher Von Dollen, Tianyi Wang, Remus Wong, Yijie Xu, Noah Young, Karen Zeller, Allen Zhan.

1 Institute for Systems Genetics and Department of Biochemistry and Molecular Pharmacology, NYU Langone Health, New York, NY 10016, USA
2 Department of Environmental Health and Engineering, Bloomberg School of Public Health, Johns Hopkins University, Baltimore, MD 21205, USA
3 European Molecular Biology Laboratory (EMBL), Genome Biology Unit, 69117 Heidelberg, Germany
4 School of Biological Sciences, The University of Edinburgh, Edinburgh EH9 3BF, UK
5 School of Informatics, The University of Edinburgh, Edinburgh EH8 9AB, UK
6 Department of Biomedical Engineering, Whiting School of Engineering, Johns Hopkins University, Baltimore, MD 21218, USA
7 Department of Biology, Krieger School of Arts and Sciences, Johns Hopkins University, Baltimore, MD 21218, USA
8 Department of Chemical and Biomolecular Engineering, Whiting School of Engineering, Johns Hopkins University, Baltimore, MD 21218, USA
9 Laboratory of Cellular and Structural Biology, Rockefeller University, New York, NY 10065, USA
10 European Research Institute for the Biology of Ageing, University Medical Center Groningen, Groningen, the Netherlands
11 Department of Pathology, Massachusetts General Hospital, Harvard Medical School, Boston, MA 02114, USA
12 Department of Medicine/Division of Infectious Diseases, Johns Hopkins University School of Medicine, Baltimore, MD 21205, USA
13 High Throughput Biology Center, Johns Hopkins University School of Medicine, Baltimore, MD 21205, USA
14 Stanford Genome Technology Center, Stanford University, Palo Alto, CA 94304, USA
15 Department of Genetics, School of Medicine, Stanford University, Stanford, CA 94305, USA
16 Department of Biomedical Engineering, NYU Tandon School of Engineering, Brooklyn, NY 11201, USA
17 Present address: L'Oréal Research and Innovation, Clark, NJ 07066, USA
18 Present address: Pondicherry Biotech Private Limited, Pondicherry Engineering College Campus, East Coast Road, Pillaichavady, Puducherry 605014, India
19 Present address: Department of Biostatistics, Harvard T.H. Chan School of Public Health, Boston, MA 02115, USA
20 Present address: Neochromosome, Inc., Long Island City, NY 11101, USA
21 Present address: Center for Scientific and Industrial Research, Institute of Genomics & Integrative Biology, Sukhdev Vihar, Mathura Road, New Delhi 110025, India
22 These authors contributed equally
23 Lead contact
*Correspondence: weimin.zhang@nyulangone.org (W.Z.), jef.boeke@nyulangone.org (J.D.B.), chandra@jhmi.edu (S.C.)

Summary

We describe the complete synthesis, assembly, debugging, and characterization of a synthetic 404,963 bp yeast chromosome, *synIX*. Combined chromosome construction methods were used to synthesize and integrate the left arm of *synIX* (*synIXL*) into a strain containing previously described *synIXR*. During *synIX* strain characterization, we identified and resolved a bug related to *EST3*, a gene involved in telomerase function, producing a *synIX* strain with near wild-type fitness. To facilitate future synthetic chromosome consolidation and increase flexibility of chromosome transfer between distinct strains, we combined chromoduction, a method to transfer a whole chromosome between two strains, with conditional centromere destabilization to substitute a chromosome of interest for its native counterpart. We found that both *synIX* transfer via chromoduction and wild-type *IX* destabilization were efficient methods. We observed that wild-type *II* tended to co-transfer with *synIX* and was co-destabilized with wild-type *IX*, suggesting a potential gene dosage compensation relationship between these two chromosomes.

Keywords: *Saccharomyces cerevisiae*, *synIX*, megachunk assembly, chromosome debugging, *EST3*, chromoduction, chromosome substitution, centromere destabilization, transcriptomics

Introduction

The Synthetic Yeast Genome Project (Sc2.0) marks a key milestone in the development of "designer" eukaryotic genomes. This global effort seeks to produce a modified version of the ~12 Mb *Saccharomyces cerevisiae* genome from the bottom up that retains native strain fitness while eliminating repetitive elements to improve genome stability and adding custom features to endow new genome functionalities. These changes include deletion of tRNA genes and introduction of loxPsym sites (nondirectional loxP sites that, being symmetric, can recombine with each other in two distinct orientations) downstream of non-essential genes, enabling genome rearrangement via the SCRaMbLE (Synthetic Chromosome Rearrangement and Modification by LoxP-mediated Evolution) system and subsequent study of how different DNA sequence changes affect organismal fitness and function.[1-4] More broadly, by establishing a set of common design principles for all sixteen yeast chromosomes, Sc2.0 aims to provide a blueprint for future eukaryotic genome engineering endeavors. As part of this project, each chromosome in the yeast genome has been redesigned and built from synthesized blocks of DNA. Following the previous construction of several synthetic chromosomes, we report the assembly and characterization of synthetic chromosome *IX* (*synIX*), coinciding with completion of the assembly phase of the Sc2.0 project as a whole.[5-17]

Our group initially assembled a circular version of the right arm of the chromosome, *synIXR*, as a proof-of-principle for feasibility of the Sc2.0 project,[6] and subsequently incorporated that chromosome arm into an otherwise wild-type and linear version of chromosome *IX.*[2] Here, we describe the construction and characterization of the left arm of chromosome *IX*, *synIXL*, and consequently, the completion of *synIX* in its entirety. As with many of the other completed Sc2.0 chromosomes and in accordance with the Sc2.0 project objectives, *synIX*-containing strains, following a "debugging" process to resolve any deficiencies in fitness across multiple growth conditions, behave similarly to the ancestral BY4741 yeast strain with respect to growth fitness and transcriptional profiling.

Over the past decade, fitness defects have emerged during completion of many of the Sc2.0 chromosome strains. We attribute these growth issues, or "bugs," to our incomplete understanding of *Saccharomyces cerevisiae* and its genome during the project's initial design phase. Identifying and resolving such problems may improve future genome engineering efforts and help us anticipate and avoid potential complications. More specifically, bugs in previous Sc2.0 strains have commonly arisen from design choices (sequence additions, deletions, or alterations) that unexpectedly affect protein or RNA levels. For example, PCRTag recoding (intended to alter DNA sequence without changing the resulting amino acid sequence, producing a watermark to distinguish synthetic and wild-type sequences) has lowered protein expression or interfered with transcription factor binding sites in other synthetic chromosome strains.[7,9,11,12] Addition of loxPsym sites and removal of introns as part of synthetic chromosome design have also affected RNA expression of genes in Sc2.0 strains, altering strain fitness.[7,11] In the case of *synIX*, we identify and characterize a fitness defect related to a sequence adjacent to the *EST3* gene, one of the components of yeast telomerase holoenzyme that is involved in yeast telomere replication.[18-20] We show that this was the consequence of a specific intentional design step, namely removal of a

tRNA gene and associated repetitive DNA sequences. Deletion of a tRNA gene, Ty1 retroelement, and the DNA between them led to reduced average telomere length and impaired the *synIX* strain's ability to grow at higher temperature (37°C), a likely consequence of significant Est3p reduction. Reintroduction of part or all of this sequence dramatically improved strain fitness, with associated partial or complete restoration of telomere length and Est3p levels depending on sequence composition and variable effects on the strain's transcriptional profile.

The ultimate goal of Sc2.0 is to create a high-fitness yeast strain with a fully synthetic genome. A previously described chromosome consolidation method that relies on chromosome endoreduplication followed by sporulation becomes laborious and time-consuming as the synthetic chromosome number increases in the strain.[2,21] Here we present a strategy which combines chromoduction of the chromosome of interest and subsequent loss of the native counterpart to accelerate consolidation. This approach takes advantage of a karyogamy defect that arises when either parent in a yeast mating has a *kar1-1* mutation.[22] Such crosses yield heterokaryons consisting of nuclear material from one yeast strain plus a mixed cytoplasm of both parental strains. In rare cases, whole chromosomes can transfer between strains following a *kar1-1* x *KAR1* cross.[23] While chromoduction occurs more frequently with smaller chromosomes than with larger ones,[23] prior work has often employed a selection strategy to identify chromoductants in which a particular chromosome of interest has been transferred.[24,25] Conversely, whole chromosome destabilization can be achieved by activating a *GAL* promoter immediately upstream of yeast centromeres.[7,26] Here, we demonstrated the feasibility of synthetic chromosome transfer using *synIX*, and produced a final haploid yeast strain in which *synIX* has replaced wild-type chromosome *IX*. This represents a promising proof-of-principle for targeted transfer of chromosomes among yeast strains; indeed, this method is in active use to perform the final consolidation of Sc2.0 chromosomes into a single yeast strain.[21]

Results

Design and assembly of *synIX*

The design of *synIX* adheres to the same principles used for the Sc2.0 project.[2] The designed sequence for *synIX* contains a variety of modifications, including deletion of ten tRNA genes (relocated to a separate tRNA neochromosome) and 11,632 bp of repetitive DNA, recoding of 54 stop codons from TAG to TAA, 436 bp of restriction enzyme sites, and 7,943 bp of PCRTags (recoded DNA sequences designed to distinguish between synthetic and native DNA without altering the resulting amino acid sequence), and addition of 142 loxPsym sites downstream of nonessential genes that allow for the Cre-mediated SCRaMbLE evolution system (**Figure 1A**).[1-4] These changes reduced the total size of chromosome *IX* from a wild-type length of 439,885 bp to a synthetic length of 404,963 bp.

Following the synthesis of *synIXR*,[6] we began construction of *synIXL* using a strain containing a linear, partially synthetic chromosome *synIXR* in which the left arm was in a native state (yLM461).[2] Assembly of *synIXL* proceeded in several stages (**Figure 1B**). Initially, we assembled 750 bp building blocks from synthetic 60-70 bp oligonucleotides through polymerase cycling assembly (PCA) in the context of the Build A Genome undergraduate class (**Figure S1A**).[5,6] We

then combined these building blocks to form 2-4 kb minichunks. In later stages of the project, as DNA synthesis technology improved and costs dropped, we obtained the remaining minichunks directly from a DNA synthesis vendor.

We divided *synIXL* into nine 30-60 kb megachunks, each made up of a series of minichunks that overlapped adjacent ones. To assemble the first six megachunks (megachunks A-F), we transformed component minichunks into our entry strain one megachunk at a time, including an auxotrophic marker added to the final minichunk of each region (**Figure 1C**). Through yeast homologous recombination, each assembly step overwrote the wild-type chromosome segment and auxotrophic marker attached to it with the synthetic segment and a new auxotrophic marker in accordance with the Switching Auxotrophies Progressively for Integration (SwAP-In) method,[2,6] enabling selection of strains containing newly integrated DNA (**Figure 1C**, **Table S1**). After each round of integration, the PCRTag watermarking system allowed identification of colonies containing desired synthetic DNA and lacking corresponding wild-type *chrIX* DNA (**Supplementary File 1**).

The minichunk integration approach used in the assembly of megachunks A-F of *synIXL* left some unwanted patches of wild-type *chrIX* sequence (**Figure 1B, top**). To improve the efficiency of synthetic DNA incorporation and to avoid such wild-type DNA patches, later portions of *synIXL* used the "megachunk cloning" integration strategy.[12] For these sections of the chromosome, we first assembled minichunks into 40-60 kb megachunks (megachunks G-I) as extrachromosomal plasmids in yeast, with an assembly success rate of approximately 20-45% (**Figure 1D, Table S2**), and subsequently transformed them into *E. coli* for plasmid extraction. Following sequence verification of the megachunks, these larger assembled pieces were released from their plasmid backbones using restriction enzyme digestion, and delivered directly into our semisynthetic (A-F) *synIX* strain for SwAP-In. We verified successful integration of the three megachunks via PCRTagging analysis and whole genome sequencing. All three megachunks constructed in this manner were integrated into the *synIX* strain in their entirety and lacked novel mutations (**Figure 1B, middle**).

To convert the wild-type DNA patches seen in megachunks A-F of *synIXL* to synthetic, we used a CRISPR-Cas9 editing strategy to selectively target *synIX* at residual *chrIX* PCRTags within each patch (**Figure S1B**) and repair these sequences with appropriate synthetic donor DNAs.[9,10] Following replacement of ten minichunks over seven rounds of CRISPR-mediated editing, we obtained a version of *synIX* that contained all the synthetic minichunks included in the chromosome's design (**Figure 1B, bottom, Table S3**).

We continued CRISPR-mediated editing of this draft strain to correct point mutations, small deletions, and duplications in *synIX*, as detailed in **Table S4**. Additionally, we discovered a discrepancy that stemmed from inaccuracies in the wild-type yeast reference genome sequence that had originally been used for synthetic chromosome design. In *synIX*, the designer sequence for the non-essential *FAA3* gene contained an extra seven base pairs missing from the most recent version of the wild-type reference sequence, resulting in a frameshift (**Figure 1E**).[27,28] A previous genetic screen linked the *faa3Δ* null allele to decreased vegetative growth;[29]

consequently, we restored proper *FAA3* function in our *synIX* strain by deleting the unwanted sequence via CRISPR-mediated editing, reestablishing the normal reading frame of *FAA3* (**Figure S2**).

During this editing process, we unexpectedly identified whole-chromosome disomy of *synIX* (**Figure 1F, top**). To restore the normal karyotype of the *synIX* strain, we integrated a *URA3-pGAL* cassette upstream of *CEN9* into one *synIX* copy,[26] induced chromosome destabilization and loss via growth in media containing galactose, and then selected against the *URA3* marker to identify strains with a single copy of *synIX* (**Figure S3**). Whole genome sequencing confirmed that the resulting *synIX* strain contained approximately equal read depth for each chromosome, as expected for a monosomic haploid yeast strain (**Figure 1F, bottom**). There were no overt phenotypic differences between the disomic and monosomic strains, suggesting that the disomy was an inadvertent consequence of CRISPR-mediated editing rather than selection for a second copy of *synIX* due to haploinsufficiency. This monosomic strain was used for further debugging.

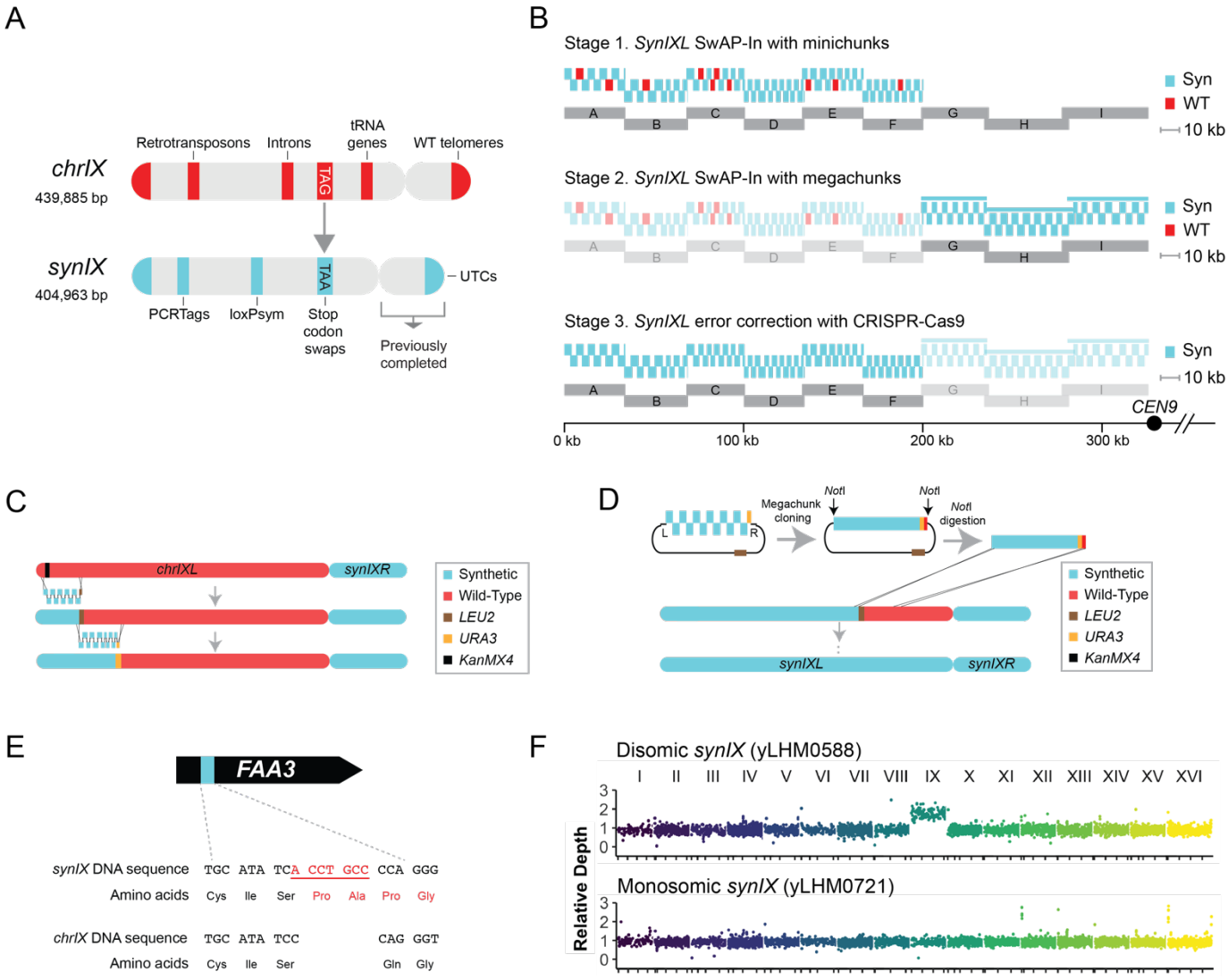

Figure 1. Design and assembly of *synIX*. (**A**) Diagram of the differences between wild-type (WT) *chrIX* and *synIX*. Designer features specific to *synIX* include the addition of PCRTags and loxPsym sites, the recoding of TAG stop codons to TAA, the replacement of wild-type telomeres with universal telomere caps (UTCs), and the removal of tRNA

genes (relocated to a tRNA neochromosome), introns, retrotransposons, and subtelomeric repeats. (**B**) Schematic of the *synIXL* construction process, reflecting the synthetic and (unwanted) WT composition of chromosome *IX* in the *synIX* strain after each stage of assembly. Stage 1: SwAP-In with minichunks (A-F). Stage 2: SwAP-In with pre-assembled megachunks (G-I, opaque with blue lines). Stage 3: Error correction with CRISPR-Cas9 (primarily in highlighted megachunks A-F). Blue: syn minichunks, red: WT minichunks, gray: megachunks. Red patches in stages 1 and 2 reflect segments of DNA that were not replaced by their expected synthetic MC counterparts during SwAP-In with minichunks in stage 1 (A-F); appropriate synthetic sequences were integrated at these sites during stage 3. (**C**) Minichunk integration strategy for assembling megachunks A-F of *synIX* in yeast (used for stage 1 in (**B**)). A kanMX marker (black) was integrated into the left end of wild-type *chrIX* (red). Individual minichunks (blue, synthetic) comprising one megachunk were then co-transformed into the in-progress *synIX* strain and used to overwrite the wild-type *chrIX* sequence (red) via homologous recombination. Alternating auxotrophic markers (*LEU2*, brown, and *URA3*, orange) were used and overwritten at each step, allowing for selection of the new marker and counterselection against the previous round's marker. (**D**) Megachunk plasmid assembly and integration approach for building and integrating megachunks G-I in *synIX* (used for stage 2 in (**B**)). Minichunks (blue) were assembled in yeast, and an auxotrophic marker (here, *URA3*, orange) was added to the end of each assembly, followed by a segment of *chrIX* homology. The megachunk assemblon overwrote the prior round auxotrophic marker (brown, *LEU2*) and wild-type DNA (red) by homologous recombination. (**E**) Schematic depicting a frameshift mutation in the *FAA3* gene in the *synIX* design. The synthetic sequence included seven base pairs not present in the S288C wild-type yeast reference genome. The added bases, shown in red, cause a frameshift, with the resulting *synIX* amino acid sequence (red) varying from the expected *chrIX* amino acid sequence (black, bottom). (**F**) Coverage plots showing read depth along each yeast chromosome in disomic *synIX* strain yLHM0588 (top) and monosomic *synIX* strain yLHM0721 (bottom). X axis: Yeast chromosome (not to scale). Y axis: Relative depth based on number of reads at each position divided by average read depth across the sixteen yeast chromosomes.

Debugging of *synIX*

After correcting the above *synIX* sequence issues, we found that this strain, coined yeast_chr09_9_1 (also referred to as yLHM1192), grew more poorly than the parental BY4741 strain under high-temperature (37°C) conditions on both dextrose-containing (YPD) and glycerol-containing (YPG) media (**Figure 2A**). A similar phenotype was observed in additional strain isolates equivalent to yLHM1192 (**Figure S5**). Following a pooled sequencing bug mapping method,[9] we backcrossed our *synIX* strain to a wild-type strain to generate a heterozygous diploid yeast strain for sporulation, and subsequently dissected tetrads. The goal of this process was to obtain spores containing a randomized mixture of recombinant *synIX* and *chrIX* DNA as a consequence of meiotic recombination (**Figure S4A**). By conducting whole genome sequencing of healthy and sick spores, we identified a region spanning from approximately 15-20 kb upstream of *CEN9* to 5 kb downstream of *CEN9* that appeared to be associated with our *synIX* fitness defect (**Figures 2B, S4B)**. Consistent with this region's involvement in *synIX*'s growth deficiency, our *synIX* strain initially exhibited a marked decline in fitness on YPD at 37°C following the integration of megachunk I, which contained the synthetic sequence corresponding to this portion of the chromosome (**Figure S6)**. To determine the gene responsible for the bug within this ~20-25 kb region, we assembled the wild-type version of each of the genes in this region into a *CEN* plasmid for complementation (**Figure S7**). The strains containing a plasmid with *EST3* showed a pronounced improvement in fitness on both YPD and YPG at 37°C compared with the buggy *synIX* strain (**Figures 2B, S7**).

To investigate which modifications of the synthetic *EST3* gene might contribute to this fitness defect, we replaced sections of the synthetic region with corresponding wild-type sequences in our *synIX* strain and monitored strain fitness. Replacing the coding sequence of *EST3* was insufficient

to restore fitness on YPD or YPG at 37°C (**Figure 2C, yLHM1429)**; however, restoring both a deleted segment containing an aspartyl tRNA gene and a nearby Ty1 long terminal repeat (LTR) element dramatically improved *synIX* strain fitness on both YPD and YPG at 37°C (**Figure 2C, yLHM1430 and yLHM1431)**. To better assess the contributions of these *EST3*-adjacent elements to strain fitness, we next introduced smaller modifications to *EST3*'s upstream region in the *synIX* strain, including different combinations of the aspartyl tRNA gene, nearby Ty1 LTR, and an intervening single-copy "gap" DNA sequence with no known function that separates the tRNA gene and Ty1 LTR in the native *chrIX* sequence (**Figure 3A, Table S5**). We found that all of these edits improved strain growth fitness (**Figure 3A**). Similar phenotypes were observed in additional strains generated for each modification, and did not noticeably change following extended strain passaging (**Figure S8**).

As *EST3* is involved in telomere maintenance, we hypothesized that *EST3*-associated changes in fitness might correlate with changes in average strain telomere length. Consequently, we next assessed telomere length of our *synIX* and variant strains via Southern blotting with a probe specific for telomeric repeats (**Figure 3B**). Following enzymatic digestion of yeast gDNA with *Xho*I, a smear of telomeric fragments from chromosome ends containing Y' elements can be seen at the bottom or each lane; these fragments were used to estimate average telomere length, with other telomeric fragments appearing at larger sizes in each lane. As expected, yLHM1192's telomeres were markedly shorter than those seen in the wild-type BY4741 strain. Interestingly, however, the telomeres in the modified *synIX* strains split into two length groups; three groups of strains, yLHM1504 (containing the entire tRNA, intervening "gap" sequence between the tRNA and Ty1 with no known function, and Ty1 sequence), yLHM1506 (containing the tRNA and gap sequences, but not the Ty1 sequence), and yLHM1601 (containing a tRNA with a transcription-inactivating point mutation[30-33] and the aforementioned gap sequence) had telomeres similar in length to or slightly longer than wild-type yeast, while two other groups of strains, yLHM1505 (containing just the gap sequence and Ty1 LTR) and yLHM1591 (containing just the gap sequence), had telomeres that were shorter than BY4741, but slightly longer than yLHM1192.

Next, we wanted to assess the role of these upstream *EST3* modifications on strain fitness and telomere length independent of any other *synIX*-associated strain changes. To do this, we introduced each of our synthetic modifications upstream of *EST3* (from yLHM1192, yLHM1504-1506, yLHM1591, and yLHM1601) to wild-type yeast, while otherwise maintaining the native *chrIX* sequence (**Figure 4A**). As in our *synIX* strains, the yLHM1192-equivalent wild-type edited strains showed a decline in fitness on YPG plates at 37°C, while the other modified strains showed fitness similar to wild-type BY4741 (**Figure S9**). Fitness did not change appreciably following extended strain passaging (**Figure S9**). We again examined average telomere length of these strains via Southern blot (**Figure 4B**). As with the synthetic strains, we saw three groups of telomere lengths: wild-type (BY4741, as well as the strains with the yLHM1504, yLHM1506, and yLHM1601-equivalent modifications), shortened (strains with the yLHM1192-equivalent modifications), and intermediate (strains with the yLHM1505-equivalent and yLHM1591-equivalent modifications).

We next sought to understand why all of our modifications improved strain fitness, but only some fully restored telomere length to wild-type levels. We hypothesized that differences in *EST3*

translation and/or transcription might result in variable telomere length across strains. To examine Est3p expression in our modified *synIX* strains, we tagged the 3' end of *EST3* with a 3X FLAG tag and monitored protein levels after strain growth at 37°C (**Figure 5A, Table S6**). FLAG-tagged synthetic strains were crossed to an untagged wild-type strain of opposite mating type (BY4742) to complement any other recessive *synIX*-related effects on strain growth while allowing for monitoring of Est3p production from the synthetic locus. Consistent with the telomere length data, the yLHM1504-, yLHM1506-, and yLHM1601-derived strains expressed higher levels of FLAG-tagged Est3p than did the yLHM1192-, yLHM1505-, and yLHM1591-derived strains (**Figure 5A**). A follow-up comparison of the yLHM1192-, yLHM1505-, and yLHM1591-derived strains revealed higher Est3p levels in the yLHM1505-derived and yLHM1591-derived strains than in the yLHM1192-derived strains, although all three strains had markedly lower Est3p levels than did wild-type yeast (**Figure 5B**). We saw neither longer nor shorter isoforms of FLAG-tagged Est3p associated with the low-abundance strains (**Figures 5B, S10**). Similar results were observed in FLAG-tagged heterozygous diploid strains generated by crossing FLAG-tagged versions of the wild-type *EST3* variant strains from **Figure 4A** and **Figure S9** to untagged BY4742 and monitoring Est3p levels (**Figures S11A, S11B**).

To further elucidate what might contribute to the variations in Est3p levels in our engineered *synIX* strains, we examined RNA sequencing data to look for changes in RNA expression patterns. Of note, strand-specific RNA sequencing data revealed differences in the pattern of *EST3* transcripts in the wild-type and *synIX* strains at both 30°C and 37°C (**Figures 5C, 5D, S12A, S12B**). In particular, while both strains showed sequencing read depth throughout the *EST3* coding region, the *synIX* strain contained transcripts upstream of the expected *EST3* transcription start site that were absent from the wild-type strain. Importantly, given that these transcripts were transcribed from the same strand as native *EST3*, some *EST3* transcripts might have had an extended 5' UTR, predicted to encode upstream AUG codons that would not produce functional Est3p. In our modified *synIX* strains, we saw two classes of upstream transcript profiles (**Figures 5E, 5F**). yLHM1504, yLHM1506, and yLHM1601, the three strains with wild-type-length or slightly longer telomeres, showed a relative reduction in RNA sequencing reads directly upstream of *EST3* compared with strand-specific total reads aligned to the upstream plus coding sequence of *EST3* (**Figures 5E, 5F, S13A. S13B**). By contrast, yLHM1505 and yLHM1591, the two strains with intermediate-length telomeres, still showed substantial transcript read depth upstream of *EST3*. The wild-type strains with modifications upstream of *EST3* yielded a similar transcriptional pattern (**Figures S14A, S14B)**.

Nanopore direct RNA sequencing, which evaluates full-length transcript patterns, revealed a distinct population of *EST3*-spanning transcripts in yLHM1192 containing at least one out-of-frame AUG upstream of the expected *EST3* transcription start site (**Figure 5G**). Many of these transcripts started 250-500 bp upstream of the AUG that normally gives rise to the first methionine of functional Est3p (**Figures S15**). We hypothesize that such "non-translatable" upstream transcripts fail to yield properly translated Est3p, contributing to reduced telomerase function and decreased strain fitness (**Figure S16**). By contrast, while yLHM1505 and yLHM1591 contained a few non-translatable transcripts spanning *EST3*, most of the transcripts upstream of *EST3* that were observed in these strains terminated prior to the expected *EST3* transcription start site (gray in

Figure 5G). yLHM1192, yLHM1505, and yLHM1591 all had relatively fewer full-length, presumably translatable *EST3* transcripts than did the tRNA-containing strains (yLHM1504, yLHM1506, and yLHM1601).

Taken together, these results point to a model in which upstream initiated transcripts are unable to produce Est3p, and only reads initiating at or near the native transcription start site produce functional *EST3* transcripts and resulting protein. The original *synIX* strain (yLHM1192) appears to yield almost no functional Est3p, while variant strains produce either low (yLHM1505 and yLHM1591) or near-wild-type (yLHM1504, yLHM1506, and yLHM1601) Estp3 levels. However, strains with even a low level of functional Est3p and a moderate reduction in telomere length appear to surpass a threshold for maintaining normal strain fitness. Thus, our three classes of Est3p levels and telomere length yield only two fitness profiles; healthy strains and sick ones.

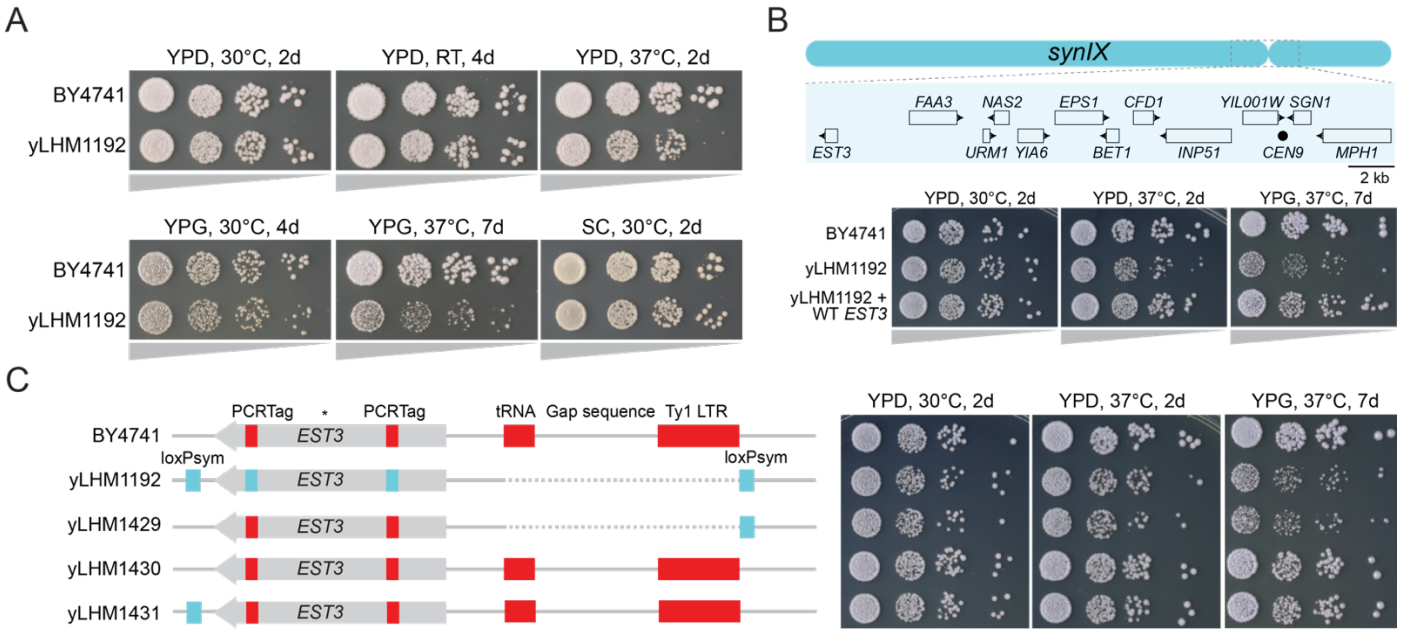

Figure 2. Identifying and mapping an *EST3*-related bug. (**A**) Spot assays comparing the growth of BY4741 (wild-type) to yLHM1192 (synthetic) across a variety of growth conditions. Each column represents a tenfold dilution. RT: Room temperature, approximately 22°C. (**B**) (Top) Schematic of region near *CEN9* identified as containing the gene responsible for a *synIX* fitness defect. The unhealthy *synIX* strain (yLHM1192) was transformed with plasmids containing transcription units for each of the genes shown. (Bottom) Spot assays comparing the growth of BY4741 and yLHM1192 to yLHM1192 transformed with a plasmid containing the *EST3* coding sequence plus 500 bp of upstream sequence and 200 bp of downstream sequence. Each column represents a tenfold dilution. (**C**) Spot assays comparing growth of strains with different combinations of synthetic and wild-type features in and upstream of *EST3*. Each column represents a tenfold dilution. Schematics on left illustrate wild-type (red) and synthetic (blue) features present in each strain. The asterisk (*) marks the site of a programmed +1 ribosomal frameshift during *EST3* translation.

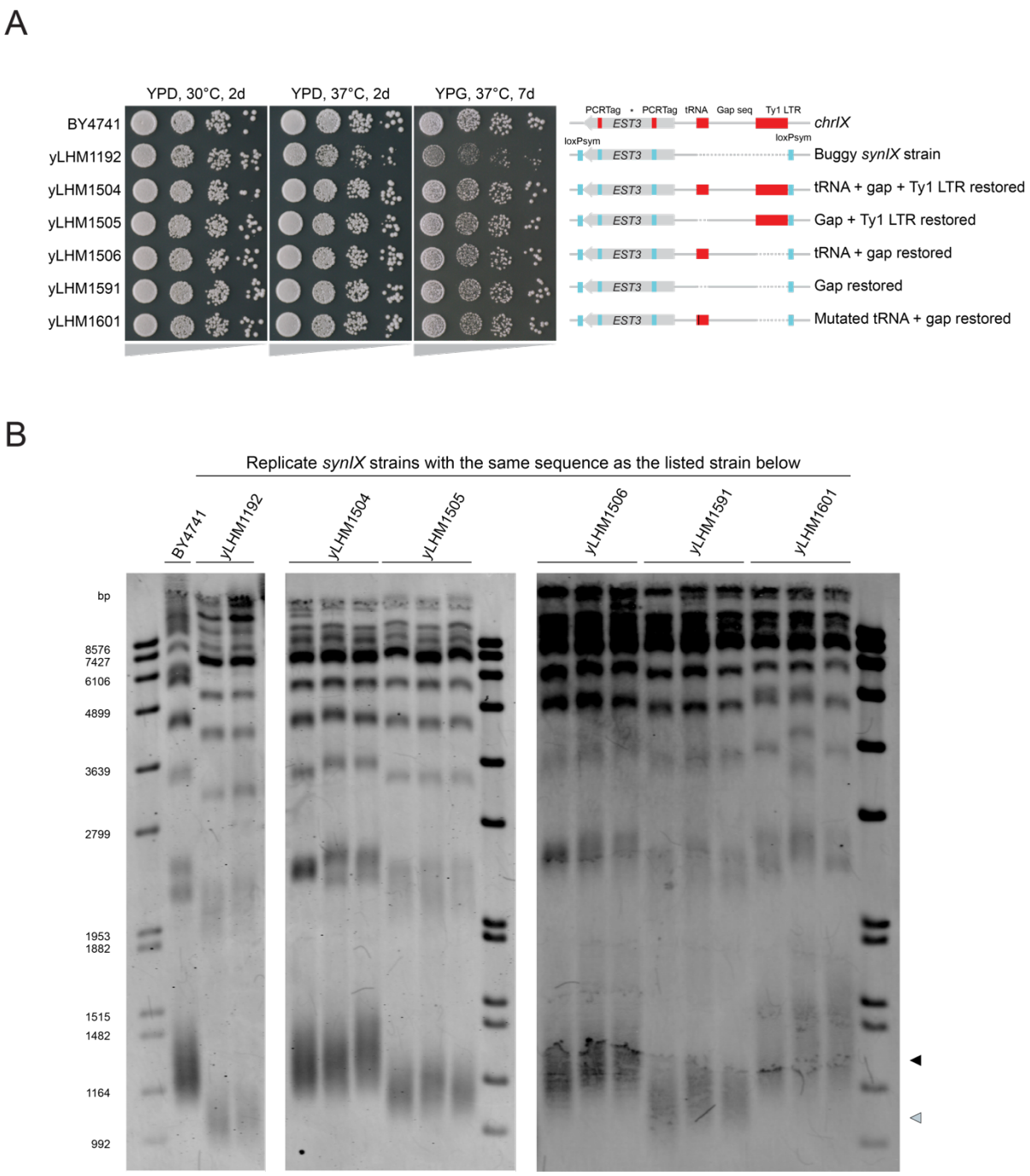

Figure 3. Modifying *synIX* strains upstream of *EST3* alters fitness and telomere length. (**A**) Spot assays and accompanying schematics of the region upstream of *EST3* for strains BY4741 (wild-type *chrIX*), yLHM1192 (synthetic), and variant strains derived from yLHM1192. Wild-type PCRTags, tRNA gene (Asp), and Ty1 long terminal repeat (LTR) are depicted in red, synthetic PCRTags and loxPsym sites in blue, mutation in $tRNA^{Asp}$ gene as a vertical black line. Each spot assay column represents a tenfold dilution. (**B**) Southern blot of *Xho*I-digested yeast gDNA derived from BY4741 (wild-type) and replicate strains with modifications equivalent to yLHM1192 (synthetic) and variant strains (yLHM1504, yLHM1505, yLHM1506, yLHM1591, and yLHM1601, as depicted in (**A**)). DNA was probed with a digoxigenin-labeled fragment specific for telomeric repeats. Black arrow (right): Average size of Y'-containing telomeric fragments for BY4741. Gray arrow (right): Average size of Y'-containing telomeric fragments for yLHM1192. Left and middle panels: Left and right halves of one Southern blot, cropped to remove one lane in the middle. Right panel: Right side of a second Southern blot, cropped to remove left-hand ladder, BY4741, and yLHM1192 lanes.

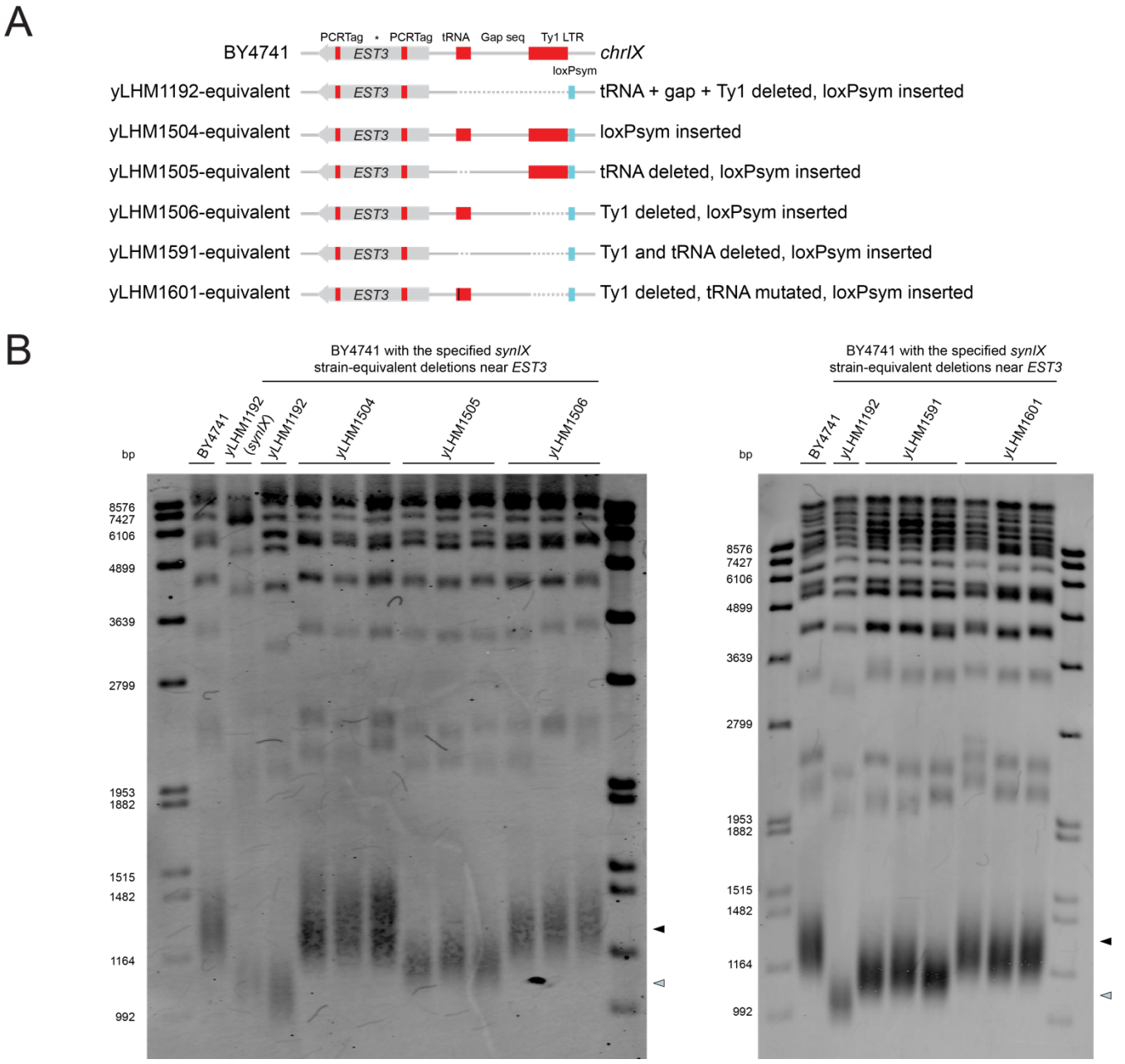

Figure 4. Modifying wild-type yeast strains upstream of *EST3* alters telomere length. (**A**) Schematics of the region upstream of *EST3* for strains BY4741 (wild-type *chrIX*), yLHM1192-equivalent (synthetic modification matching yLHM1192 in an otherwise wild-type yeast strain), and variant strains derived from the yLHM1192-equivalent strain. Wild-type PCRTags, tRNA gene (Asp), and Ty1 long terminal repeat (LTR) are depicted in red, loxPsym sites in blue, mutation in $tRNA^{Asp}$ gene as a vertical black line. (**B**) Southern blot of *Xho*I-digested yeast gDNA derived from BY4741 (wild-type), yLHM1192 (synthetic), and replicate strains with synthetic-equivalent modifications made upstream of *EST3*, as depicted in (**A**)). DNA was probed with a digoxigenin-labeled fragment specific for telomeric repeats. Black arrow (right): Average size of Y'-containing telomeric fragments for BY4741. Gray arrow (right): Average size of Y'-containing telomeric fragments for BY4741 + yLHM1192-equivalent deletion strain.

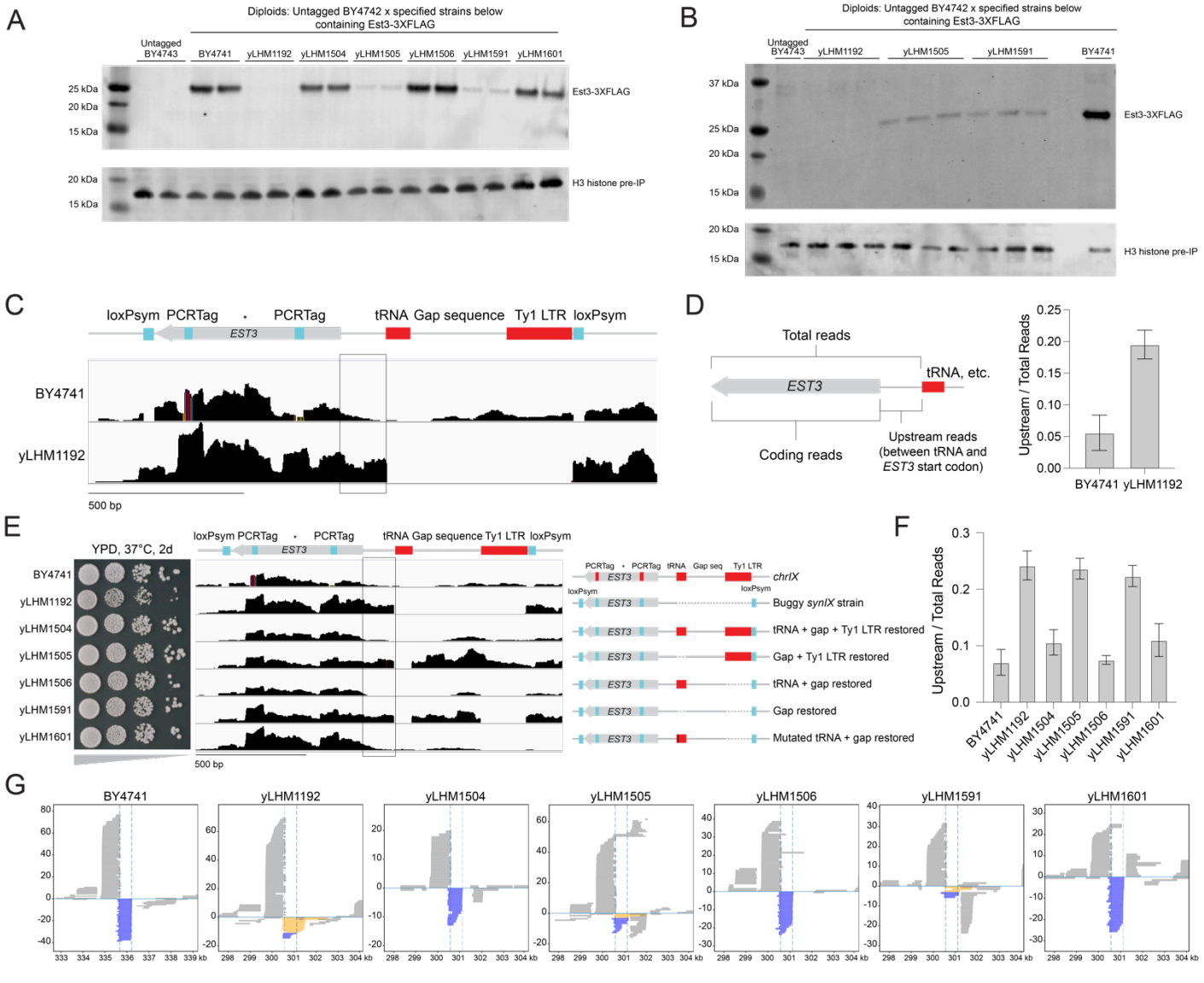

Figure 5. Dissecting the effects of *EST3*-adjacent features on *EST3* protein and RNA expression. (**A**) Immunoblotting for immunoprecipitated (IP) Est3p (top) and H3 histone pre-IP loading control (bottom). Est3p was C-terminally tagged with 3X FLAG in each synthetic strain, and diploids were generated via mating with wild-type BY4742. Two independent colonies were grown in YPD at 37°C for each strain. Right-most lane (second ladder) was cropped out of image. (**B**) Immunoblotting for immunoprecipitated (IP) Est3p (top) and H3 histone pre-IP loading control (bottom) for low-expressing Est3p strains plus controls. Est3p was C-terminally tagged with 3X FLAG in each synthetic strain, and diploids were generated via mating with wild-type BY4742. Three independent colonies were grown at YPD at 37°C for each yLHM1192-, yLHM1505-, and yLHM1591-derived diploid strain. Right-most lane (second ladder) was cropped out of image. (**C**) Strand-specific RNA sequencing alignments for the reverse strand of BY4741 and yLHM1192 (strand from which *EST3* transcription is expected, i.e., "reverse strand reads") grown at 37°C in YPD to a composite reference containing both synthetic and native *IX* features. Schematic on top illustrates wild-type *chrIX* (red) and synthetic (blue) features. Black box on the RNA sequencing alignment plot highlights region between the expected *EST3* start codon and the upstream tRNA. The asterisk (*) marks the site of a programmed +1 ribosomal frameshift during *EST3* translation. (**D**) Quantification of reverse strand reads mapping directly upstream of *EST3* (between tRNA and start codon, corresponding to black box in **C**) as a fraction of the total reverse strand *EST3* coding and upstream reads for each strain shown in **C**. Read counts based on alignment to native (BY4741) or synthetic (yLHM1192) reference sequence. Error bars represent standard deviation of three biological replicates. (**E**) Spot assays and strand-specific RNA sequencing alignments for the reverse strand reads aligning to the *EST3* region for samples grown at 37°C on YPD plates or in YPD liquid media. Strains: BY4741 (wild-type *chrIX*), yLHM1192 (synthetic), and variant strains derived from yLHM1192. Wild-type PCRTags, tRNA gene (Asp), and Ty1 long terminal repeat (LTR) are

depicted in red, synthetic PCRTags and loxPsym sites in blue, mutation in $tRNA^{Asp}$ gene as a vertical black line. Black box on the RNA sequencing alignment plot highlights region between the expected *EST3* start codon and the upstream tRNA. The asterisk (*) marks the site of a programmed +1 ribosomal frameshift during *EST3* translation. (**F**) Quantification of reverse strand reads mapping directly upstream of *EST3* (between tRNA and start codon, corresponding to black box in E) as a fraction of the total reverse strand *EST3* coding and upstream reads for each strain shown in **E**. Read counts based on alignment to native (BY4741) or synthetic (yLHM1192) reference sequence. Error bars represent standard deviation of three biological replicates. (**G**) Nanopore direct RNA sequencing reads aligned to the *EST3* region (±3kb). Strains: BY4741, yLHM1192, and variant strains derived from yLHM1192, all grown at 37°C in YPD liquid media. X axis: Chromosome coordinate. Y axis: Number of reads. Forward strand reads are above the Y axis, reverse strand reads below the Y axis. Dotted lines indicate the boundaries of the *EST3* coding region. *EST3* transcripts are expected to lie on the reverse strand. Yellow reads: "Non-translatable" reads that contain at least one AUG upstream of the expected *EST3* start codon plus a minimum of 20 bp of 5' UTR sequence. Blue reads: Reads mapping to *EST3* that start no more than 20 bp upstream of the first AUG upstream of the expected *EST3* start codon, including "translatable/functional" reads spanning the entirety of *EST3* and reads starting downstream of the *EST3*-initiating AUG.

Characterization of the healthy *synIX* strain

We ultimately proceeded with the strain in which a mutated version of the deleted tRNA gene and the adjacent gap sequence were reintroduced upstream of *EST3* (yLHM1601 in **Figure 5E**). The tRNA sequence contained a point mutation previously shown to block tRNA transcription,[30-33] allowing functional tRNA relocation to a tRNA neochromosome[15] while maintaining Est3p levels similar to those of wild-type yeast (**Figure 5A**). This strain is most consistent with Sc2.0's design principles of maximizing strain fitness while eliminating repetitive elements and tRNA genes in particular. This final *synIX* version, coined yeast_chr09_9_2, grew similarly to wild-type yeast across a variety of media types and temperature conditions, as did additional sequence-matched replicate strains (**Figures 6A, S17, S18, S19**). The final strain largely matched the expected synthetic reference sequence, with slight deviations from the original design reflecting changes made during bug fixing and other minor alterations during the assembly process (**Table S7**). The final strain also showed even coverage across *synIX* and normal chromosomal copy number (**Figure 6B**). *SynIX* migrated slightly faster on pulsed-field gel electrophoresis (PFGE) than did native *IX* (**Figure 6C**). We also observed an unusual banding pattern among a couple of the higher bands in yLHM1601, possibly related to an expanded repetitive sequence near the telomere of chromosome *XVI*. This difference did not appear to affect strain fitness, and disappeared following *synIX* transfer to an alternative matched-background wild-type yeast strain via the chromosome substitution method discussed in the next section (**Figure 6C, lanes 3 and 4**).

Transcriptional analysis of the completed *synIX* strain (yLHM1601, or yeast_chr09_9_2) identified a small number of differentially expressed genes compared to the wild-type strain (**Figures 6D, 6E, S20A, S20B**). Several hits found on *synIX* were located in or near telomeres, with some of these genes showing upregulation and other showing downregulation. On the left arm of *synIX*, *SOA1* (*YIL166C*) showed decreased expression in the *synIX* strain at 37°C (~5x lower than in BY4741). Several of the other genes originally found between *SOA1* and *TEL09L* in native chromosome *IX* were deleted in the *synIX* design. Consequently, we hypothesize that *SOA1* expression may be decreased due to increased silencing associated with its new position near *TEL09L*, as has been observed on other synthetic chromosomes where genes moved closer to the telomeres due to subtelomeric DNA deletion.[12] Conversely, right arm subtelomeric genes *YIR042C* and *YIR043C*

showed expression increases at 37°C (~12x increase for *YIR042C*) and both 30°C and 37°C (~15x and ~34x increases for *YIR043C*), respectively. Unlike *SOA1*, *YIR042C* and *YIR043C* were already located very close to *TEL09R* in native yeast chromosome *IX*. As a result, it is possible that the universal telomere caps introduced to *synIX* per Sc2.0 design principles failed to silence nearby genes to the same degree as the native telomeres, since the earliest version of the UTC used in this case lacked the X sequence used at the left telomere and elsewhere in the project. Since the X sequence, a known subtelomeric anti-silencing region,[34] is present in the native *TEL09R,* its absence could explain the selectively elevated expression of these *TEL09R*-adjacent genes.

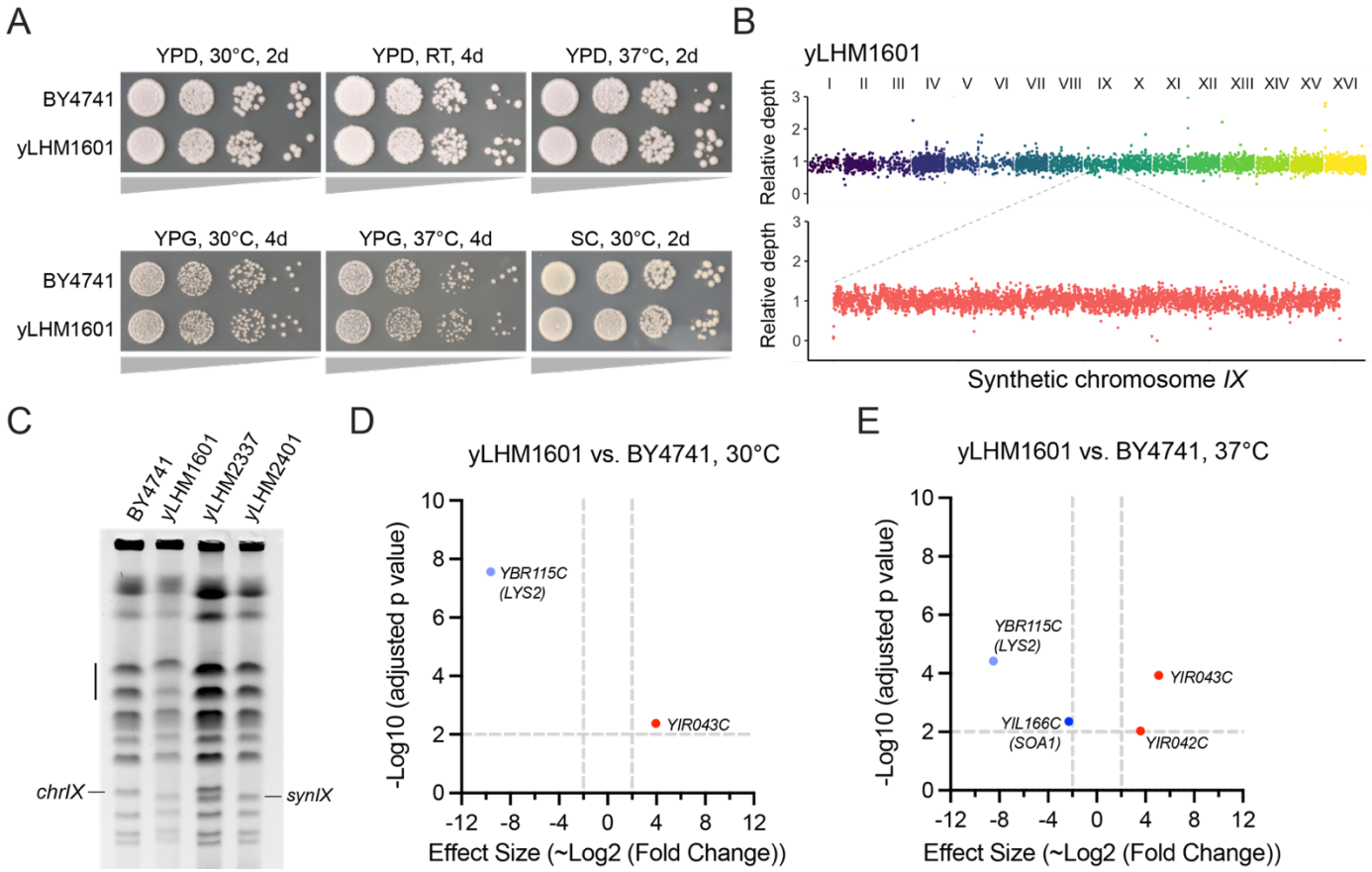

Figure 6. *SynIX* characterization. (**A**) Spot assays comparing the growth of BY4741 (wild-type) to yLHM1601 (synthetic) across a variety of temperature conditions. Each column represents a tenfold dilution. RT: Room temperature, approximately 22°C. (**B**) DNA sequencing coverage plot for *synIX* strain (yLHM1601). X axis: Yeast chromosome (not to scale), or coordinate along *synIX*. Relative depth (Y axis) based on reads mapped to the yeast_chr09_3_55 reference sequence divided by the average read depth across the sixteen yeast chromosomes (top) or *synIX* (bottom). (**C**) Pulsed-field gel showing chromosomes from BY4741 (*chrIX*), yLHM1601 (*synIX*), yLHM2337 (BY4742-background strain with copies of *chrIX* and *synIX*), and yLHM2401 (yLHM2337 after loss of *chrIX*) strains. Vertical black line indicates the location of a potential discrepancy in band intensity for larger chromosomes between BY4741 and yLHM1601; *synIX* was moved to an alternative strain (yLHM2337) with larger bands resembling BY4741 in intensity, and *chrIX* was subsequently lost from this strain (producing yLHM2401) via the strategy described in the next section. (**D-E**) Volcano plots of differentially expressed genes obtained from RNA sequencing data for *synIX* strain (yLHM1601) vs. BY4741 measured at 30°C (**D**) and 37°C (**E**) in YPD. Upregulated genes in yLHM1601 are depicted in red (chromosome *IX*), downregulated genes in medium blue (chromosome *IX*) or light blue (other chromosomes). Transcript counts are based on alignment to the S288C reference transcriptome. Auxotrophic gene *LYS2* was present in BY4741, but not yLHM1601. Fold change cutoff is 4, adjusted p-value cutoff is 0.01. Three

biological replicates were used for each strain. For corresponding unfiltered plots of RNA sequencing data depicting all measured genes, see **Figures S21A** and **S21B**.

Chromosome substitution of *synIX*

Here, we sought to combine chromoduction with subsequent loss of the corresponding native chromosome from the recipient strain to seamlessly move *synIX* between yeast strains while maintaining normal karyotype in the final strain of interest (**Figure 7A**). As a proof-of-concept, a disomic *synIX* strain was used as the donor, as an extra copy of *synIX* was deemed likely to produce higher chromosome transfer efficiency.[24] A *kar1-1* mutant strain was used as the recipient strain for blocking karyogamy during mating. Notably, the recipient strain also contained two mutations, *can1* and *cyh2*, as recessive selectable markers to ensure robust exclusion of donor cells or potential diploid cells on canavanine- and cycloheximide-containing medium. To facilitate selection of recipient strains containing *synIX* transferred from the donor strain following strain crossing, we deleted the *LYS12* gene on the recipient strain's wild-type chromosome *IX* (**Figure S21A**). This allowed facile selection for lysine prototrophy to ensure *synIX* was present in the chromoductants. Additionally, to enable eventual loss of the wild-type *chrIX* from the recipient strain, we subsequently knocked in a *URA3-pGAL* cassette upstream of *CEN9* in the recipient strain for *chrIX* destabilization and counterselection (**Figure S21B**).[26]

After modifying the recipient strain, we mated the donor and recipient strains (yLHM0387 and yWZ601, respectively) and selected for recipient cells that had acquired at least one copy of *synIX* via chromoduction on SC–Lys–Arg+canavanine+cycloheximide plates. A PCRTagging assay was performed using selected PCRTags across *chrIX* and *synIX*. Four chromoductants (yWZ610-613) containing both *chrIX* and *synIX* PCRTag amplicons were isolated from 14 candidates (**Figure S21C**). Disomic chromoductants stably maintained both *chrIX* and *synIX* after restreaking onto fresh lysine-deficient plates. Genotyping validation of the four disomic chromoductants suggested that yWZ612 and yWZ613 had additionally acquired the *HIS4* gene on chromosome *III* from the donor strain (the recipient strain was *his4Δ0*), suggesting chromosome *III* was co-transferred along with *synIX* **(Figure S21D)**.

We next sought to destabilize *chrIX* in the disomic chromoductants to generate haploid strains with a single copy of *synIX*. We grew the disomic chromoductants (yWZ610, yWZ611) in galactose-containing media to activate transcription of the *GAL* promoter, destabilizing *CEN9* and consequently leading to *chrIX* loss during mitosis.[26] PCRTagging analysis of the resulting chromoductants (yWZ618, yWZ619) showed that only *synIX* was present (**Figure S21E**). Lastly, we subjected a series of yeast strains we generated during chromoduction to a PFGE assay. As expected, 1) *synIX* was slightly smaller than *chrIX* in both BY4741 and the recipient strain, 2) both *synIX* and *chrIX* were present in disomic chromoductants, 3) chromosome *III* was co-transferred with *synIX* in yWZ612 and yWZ613, and 4) *chrIX* was lost in chromoductants following galactose induction and counterselection against *chrIX* (yWZ618, yWZ619) (**Figure 7B**). However, we were surprised to observe that two of our chromoductants, yWZ610 and yWZ611, contained an extra copy of chromosome *II* in addition to copies of both *chrIX* and *synIX* (**Figure 7B**). Whole genome sequencing of these chromoductants confirmed these PFGE results (**Figure 7C**). However, further examination of SNPs differing between the donor and recipient chromosome *II* revealed that

yWZ610 contained one donor *II* and one recipient *II*, while yWZ611 contained two copies of recipient *II* (**Figure 7D**). This finding suggested that in yWZ611, even though chromosome *II* was not co-transferred with *synIX*, the yeast still endoreduplicated chromosome *II*, perhaps to balance the gene dosage perturbation caused by *synIX* chromoduction. Interestingly, during the inactivation of *chrIX* in the yWZ610 and yWZ611 strains, chromosome *II* was simultaneously lost as well (**Figure 7B**, yWZ618 and yWZ619).

To investigate whether the co-transfer and simultaneous loss of chromosome *IX* and *II* was coincidental, we next isolated another 11 disomic chromoductants from a repeated chromoduction experiment. Interestingly, whole genome sequencing revealed that 10 of the 11 disomic chromoductants gained an extra copy of chromosome *II* (**Figure 7E**). Following counterselection against *chrIX*, four disomic chromoductants lost chromosome *II*, while six chromoductants remained disomic (**Figure 7F**). To rule out the possibility that this phenomenon was specific to our disomic *synIX* donor strain, we performed chromosome substitution using one alternative disomic *synIX* donor strain and three monosomic *synIX* donor strains. As in earlier experiments, chromosome *II* was frequently co-transferred with *synIX*, and the extra copy of chromosome *II* often disappeared after culturing strains in galactose (**Table S8**). In conclusion, we successfully transferred *synIX* from different donor strains to a *kar1-1* recipient strain via chromoduction. More in-depth diagnosis of the chromoductants revealed that chromosome *II* was preferentially and consistently co-transferred with *synIX*, and then was frequently lost during counterselection against *chrIX*.

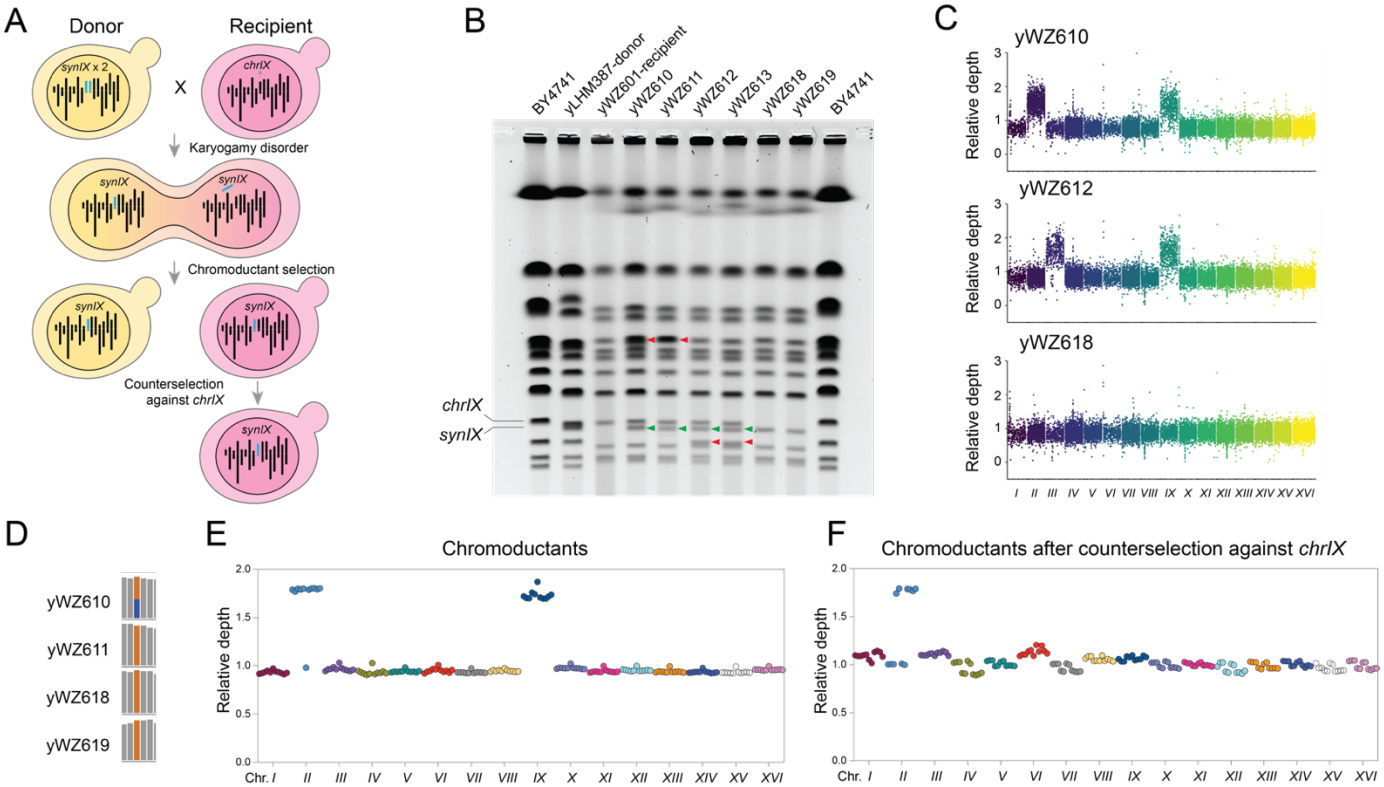

Figure 7. Chromosome substitution of *synIX*. (**A**) Chromosome substitution occurs in two steps, chromoduction, in which *synIX* is transferred to a recipient strain, followed by counterselection against wild-type *chrIX* to remove the native version of the chromosome and restore normal chromosome copy number in the chromoductant strain.

Schematic diagram of substitution steps. Black bars, wild-type chromosomes. Blue bars, *synIX*. Recipient strain harbors *ade2* mutation, and thus forms pink colonies, for easily distinguishing chromoductants. (**B**) Pulsed-field gel electrophoresis of donor strain, recipient strain, disomic chromoductants, and chromoductants after counterselection against *chrIX*. BY4741 serves as control. *ChrIX* and *synIX* chromosomes indicated with black arrows. Green triangles indicate *synIX* in disomic chromoductants. Red triangles indicate the extra chromosome *II* or chromosome *III* in disomic chromoductants. (**C**) Whole genome sequencing read depth plots of disomic chromoductants (yWZ610, yWZ612) and *chrIX* counterselected (i.e., fully substituted) chromoductants (yWZ618). X axis: Sixteen yeast chromosomes, not drawn to scale. Y axis: Relative read depth, calculated as number of reads at each position divided by average read depth across the sixteen yeast chromosomes. (**D**) Plot of SNPs on chromosome *II* in chromoductant strains before and after counterselection against *chrIX*. Recipient strain SNP highlighted in orange, donor strain SNP in blue. Strains: yWZ610: chromoductant strain with one copy of chromosome *II* from the donor strain and one from the recipient strain (mixed SNP population); yWZ611: chromoductant strain with two copies of chromosome *II* from the recipient strain (endoreduplicated *II*); yWZ618: strain derived from yWZ610 after counterselection against *chrIX*, with one copy of *II* harboring recipient strain SNP; yWZ619: strain derived from yWZ611 after counterselection against *chrIX*, with one copy of *II* harboring recipient strain SNP. (**E**) Relative depth plot for chromosome substitution strains prior to counterselection against *chrIX*. X axis: Sixteen yeast chromosomes, not drawn to scale. Y axis: Relative read depth. (**F**) Relative depth plot for chromosome substitution strains after counterselection against *chrIX*. X axis: Sixteen yeast chromosomes, not drawn to scale. Y axis: Relative read depth.

Discussion

We successfully conclude the synthesis, debugging, and characterization of *synIX*. *SynIX's* developmental history reflects advances in DNA synthesis technology over more than a decade. When the project first began, each segment of DNA was painstakingly assembled by undergraduates from oligonucleotides into minichunks, which in turn were integrated iteratively into the yeast genome to overwrite native chromosome *IX*. While such methods enabled successful incorporation of much of the synthetic sequence of interest, drawbacks included the inadvertent retention of wild-type patches and introduction of new point mutations. Newer approaches, including direct minichunk synthesis and megachunk cloning and sequencing prior to integration, greatly improved assembly efficiency and reduced construction error rates. Ultimately, we produced a yeast strain with a fully synthetic version of chromosome *IX* that displays near wild-type fitness.

While debugging *synIX*, we identified a fitness defect related to deletion of DNA sequence upstream of the *EST3* gene containing an aspartyl tRNA gene, a Ty1 LTR, and an intervening single copy DNA sequence upstream of the *EST3* gene. Strains with this deletion showed a reduction in telomere length as well as reduced Est3p levels and many RNA species mapping upstream of *EST3's* normal transcription start site. Reinserting all or part of the deleted sequence was sufficient to restore normal strain growth fitness. However, only a subset of the edited strains, specifically those containing the tRNA gene, showed a reduction in transcriptional activity upstream of *EST3* and a restoration of normal or near-normal Est3p levels and normal telomere length. We hypothesize that the tRNA sequence normally provides a buffer against production of aberrant transcripts upstream of *EST3*, and thus, the transcripts that are produced in tRNA-containing strains more effectively give rise to functional, full-length Est3p. Indeed, there is considerable evidence that tRNAs suppress transcription from nearby RNA polymerase II promoters in a process referred to as tRNA-mediated gene silencing.[33,35,36] Consistent with this idea, nanopore RNA sequencing data suggests that a subset of transcripts include one or more

AUGs upstream of *EST3*, and thus presumably fail to undergo proper translation; strains with an abundance of such transcripts also appear to have fewer full-length, translatable transcripts and lower Est3p levels. Other changes made upstream of *EST3*, such as reinsertion of the gap sequence between the tRNA and the Ty1 LTR or Ty1 LTR itself, seemingly trigger small improvements in Est3p levels vs. those found in strains with the original *synIX* design. These strains have intermediate length telomeres, longer than those seen in the original *synIX* design but shorter than those seen in native yeast, and maintain stable fitness after repeated passaging. We speculate that the changes introduced to these strains may be sufficient to maintain Est3p production and consequent telomere length above a threshold level needed for normal strain fitness, despite not fully returning either to native levels.

Interestingly, a similar occurrence of abnormal transcriptional patterns resulting from tRNA deletion and *loxPsym* site insertion was previously observed at the *HIS2* locus in *synVI*.[7] In this case, the authors suggested that a "cryptic start site" upstream of *HIS2*, generated by the altered sequence in this region, might yield a subset of transcripts incapable of producing functional His2 protein, or that this transcription might impair normal *HIS2* promoter activity. It would be useful to examine whether common principles underlie multiple Sc2.0 bugs following tRNA deletion.

Finally, we demonstrated a chromosome substitution technique that combines selective chromoduction, or movement of a desired chromosome between yeast strains, with subsequent destabilization and loss of the corresponding native chromosome. During this process of chromosome substitution, we found that certain chromosomes appeared to co-transfer with *synIX* at higher frequencies than did others. Specifically, we saw multiple instances of transfer of chromosome *II* or chromosome *III* alongside *synIX*. These extra chromosomes often disappeared following the destabilization of *chrIX*. Prior work suggested that smaller chromosomes might be more likely to transfer during chromoduction than larger ones, and that co-transfer of multiple chromosomes commonly occurs.[23] However, as chromosome *II* is not a small chromosome, it seems unlikely that chromosome size fully explains the specific co-transfer of chromosome *II*.

It is likely that an extra copy of chromosome *II* plays a role in balancing a gene dosage imbalance arising from the transient extra copy of chromosome *IX* introduced by chromoduction. In one of the chromoductant strains, analysis of SNPs from the recipient and donor strains' copies of chromosome *II* revealed that both copies of the chromosome came from the recipient strain. The presence of an endoreduplicated chromosome *II* is consistent with the hypothesis that there is selective pressure for a higher dosage of chromosome *II* fitness in the presence of two copies of chromosome *IX*, and that the co-migration of chromosomes *II* and *synIX* in the other chromoductant strains may not have occurred by chance. Moreover, multiple donor strains, including strains disomic and monosomic for *synIX*, showed co-transfer of chromosome *II* alongside *synIX*. It may be valuable to ascertain the mechanisms that dictate which chromosomes tend to co-transfer between strains during chromoduction.

Ultimately, chromosome substitution has numerous applications, including transfer and consolidation of chromosomes from other wild-type yeast strains, engineered strains, and non-laboratory strains. Existing work profiling collections of hundreds or thousands of yeast strains has

shed light on yeast diversity and evolution;[37-39] chromosome substitution will facilitate further probing of how changes on individual chromosomes or combinations of chromosomes affect strain fitness and function. Similarly, this technology could assist in analyzing why genomic changes in SCRaMbLEd yeast strains and other engineered strains produce particular phenotypic results.[1-4] More immediately, chromosome substitution is already in use to bring the initial phase of Sc2.0 to a close via the consolidation of all of the synthetic chromosomes into a single strain, marking a key eukaryotic genome engineering milestone.[21]

STAR Methods

Key resources table

REAGENT or RESOURCE	SOURCE	IDENTIFIER
Antibodies		
Digoxigenin Recombinant Rabbit Monoclonal Antibody (9H27L19)	Invitrogen	Thermo Fisher Scientific Cat# 700772, RRID:AB_2532342
Monoclonal ANTI-FLAG® M2 antibody produced in mouse	Sigma-Aldrich	Sigma-Aldrich Cat# F1804, RRID:AB_262044
Rabbit anti-Histone H3 antibody	Abcam	Abcam Cat# ab1791, RRID:AB_302613
IRDye 800CW Goat anti-Mouse IgG1-Specific	LI-COR Biosciences	LI-COR Biosciences Cat# 926-32350, RRID:AB_2782997
IRDye 680RD Goat anti-Rabbit IgG	LI-COR Biosciences	LI-COR Biosciences Cat# 926-68071, RRID:AB_10956166
Bacterial and viral strains		
EPI300 *E. coli* strain	Lucigen	EC300150
TOP10 *E. coli* strain	Boeke lab collection	
Chemicals, peptides, and recombinant proteins		
Zymolyase 20T	US Biological	Z1000
Zymolyase 100T	US Biological	Z1004
EDTA-free protease inhibitor	Roche	11873580001
Lithium acetate dihydrate	Sigma-Aldrich	L6883
Polyethylene glycol	Sigma-Aldrich	81188
Herring sperm DNA	Promega	D1816
Potassium acetate	Fisher	BP364
Zinc acetate dihydrate	Sigma-Aldrich	Z0625
(S)-(+)-Camptothecin	Sigma-Aldrich	C9911
D-Sorbitol	Sigma-Aldrich	S1876
6-Azauracil	Sigma-Aldrich	A1757
Hydroxyurea	Sigma-Aldrich	H8627
Methyl methanesulfonate	Sigma-Aldrich	129925
Methyl 1-(butylcarbamoyl)-2-benzimidazolecarbamate (Benomyl)	Sigma-Aldrich	381586
Cycloheximide	Sigma-Aldrich	01810
L-Canavanine sulfate	Sigma-Aldrich	C9758
Hydrogen peroxide	Millipore	88597
ULTRAhyb™ Ultrasensitive Hybridization Buffer	Invitrogen	AM8669
SSPE Buffer 20× Concentrate	Sigma-Aldrich	S2015
Intercept (TBS) Blocking Buffer	LI-COR Biosciences	927-60001
TWEEN 20	Sigma-Aldrich	P1379
Triton™ X-100	Sigma-Aldrich	X100
2-Mercaptoethanol	Sigma-Aldrich	M6250
GoTaq Green Master Mix	Promega	M7123
RNase A	Thermo Fisher Scientific	EN0531
*Not*I-HF	NEB	R1389L
*Bbs*I-HF	NEB	R3539L
*Afe*I	NEB	R0652L
*Xho*I	NEB	R0146L

Amino-terminal FLAG-BAP™ Fusion Protein	Sigma-Aldrich	P7582
Dynabeads™ M-270 Epoxy	Invitrogen	14302D
Dynabeads™ Oligo(dT)$_{25}$	Invitrogen	61005
SuperScript™ IV Reverse Transcriptase	Invitrogen	18090010
Agencourt RNAClean XP beads	Beckman Coulter	A63987
Critical commercial assays		
PureLink™ HiPure Plasmid Midiprep Kit	Invitrogen	K2100-15
Zyppy Plasmid Miniprep Kit	Zymo Research	D4037
Fungi/Yeast Genomic DNA Isolation Kit	Norgen	27300
Qubit dsDNA HS Assay Kit	Thermo Fisher Scientific	Q32854
Qubit dsDNA BR Assay Kit	Thermo Fisher Scientific	Q32850
NEBNext Ultra II FS DNA Library Kit	NEB	E7805
Zymo-Spin I Columns	Zymo Research	C1003
PALL 60207 Biodyne B High Sensitivity and Low Background Nylon Transfer Membrane, 0.45 µm Pore Size, 30 cm W x 3 m L Roll	Pall Corporation	60207
RNeasy Mini Kit	QIAGEN	74106
Qubit RNA BR Assay Kit	Thermo Fisher Scientific	Q10210
QIAseq Stranded Total RNA Library Kit	QIAGEN	180745
QIAseq FastSelect -rRNA Yeast Kit	QIAGEN	334217
NextSeq 500/550 High Output Kit v2.5 (75 Cycles)	Illumina	20024906
NextSeq 500/550 High Output Kit v2.5 (150 Cycles)	Illumina	20024907
MasterPure Yeast RNA Purification Kit	Lucigen	MPY03100
Agilent RNA 6000 Nano Kit	Agilent	5067-1511
Qubit RNA HS Assay Kit	Thermo Fisher Scientific	Q32852
Direct RNA Sequencing Kit	Oxford Nanopore Technologies	SQK-RNA002
Flow Cell Priming Kit	Oxford Nanopore Technologies	EXP-FLP001
MinION Flow Cell (R9.4.1)	Oxford Nanopore Technologies	FLO-MIN106D
Experimental models: Organisms/strains		
Saccharomyces cerevisiae: BY4741	Jef Boeke's laboratory	N/A
All other strains used in this study are listed in Table S1	N/A	N/A
Oligonucleotides		

PCRTag primers are listed in Supplementary File 1	N/A	N/A
Recombinant DNA		
See Tables S2-S6 for plasmids used in this study	N/A	N/A
Software and algorithms		
GeneDesign	[40]	
R	R Core Team	https://www.R-project.org/
Rstudio v1.3.1093	Rstudio	https://www.rstudio.com
Integrated Genomics Viewer (IGV) v2.7.2	Broad Institute[41]	http://software.broadinstitute.org/software/igv/
Image Studio Lite	LI-COR Biosciences	https://www.licor.com/bio/image-studio/
GraphPad Prism v9.4.0 for macOS	GraphPad Software	http://www.graphpad.com
Trimmomatic v0.39	[42]	http://www.usadellab.org/cms/index.php?page=trimmomatic
FastQC v0.11.4	[43]	http://www.bioinformatics.babraham.ac.uk/projects/fastqc/
Bowtie 2 v2.2.9	[44]	http://bowtie-bio.sourceforge.net/bowtie2/index.shtml
ggplot2 v3.3.5	[45]	https://ggplot2.tidyverse.org/
Seqtk v1.3	N/A	https://github.com/lh3/seqtk/
Kallisto v0.46.0	[46]	https://pachterlab.github.io/kallisto/
STAR v2.5.2a	[47]	https://github.com/alexdobin/STAR/
SAMtools v1.9	[48]	http://samtools.sourceforge.net/
BEDtools v2.26.0	[49]	https://github.com/arq5x/bedtools2/
sleuth v0.30.0	[50]	https://pachterlab.github.io/sleuth/
Other		
Resource website for Sc2.0	N/A	https://syntheticyeast.github.io/

RESOURCES AVAILABILITY

Lead contact

Further information should be directed to and will be fulfilled by the lead contact Jef D. Boeke (jef.boeke@nyulangone.org).

Materials availability

All unique/stable reagents generated in this study are available from the lead contact with a completed Materials Transfer Agreement.

Data and code availability

Data: All data reported in this paper will be shared by the lead contact upon request.

Code: This work did not generate any code.

Any additional information required to reanalyze the data reported in this paper is available from the lead contact upon request.

Experimental Methods

SynIX design

Design sequences for *synIX* were developed using BioStudio, according to the same guidelines used for designing the other synthetic chromosomes for Sc2.0. Designer sequences yeast_chr09_3_54 and yeast_chr09_3_55 were used as references for subsequent steps in the project. Version yeast_chr09_3_56 was developed after completion of yeast_chr09_9_02, and was used as a reference for final strain verification.

Yeast media

Yeast strains were cultured in rich medium (YPD) or synthetic complete (SC) medium with appropriate components "dropped out" e.g., SC–Ura lacks uracil. Yeast transformations were performed using lithium acetate protocols.[51] YPG plates used for growth assays contained 3% glycerol in place of dextrose as a carbon source. For expanded spot assays, the following media types were used: pH 4 and pH 8: pH of 2X YEP + dextrose adjusted using HCl and NaOH, respectively before adding agar; camptothecin (Sigma-Aldrich, C9911): 0.1 μg/mL, 0.5 μg/mL, or 1.0 μg/mL in YPD; sorbitol (Sigma-Aldrich, S1876): 0.5 M, 1.0 M, 1.5 M, or 2.0 M in YPD; 6-azauracil (Sigma-Aldrich, A1757): 100 μg/mL in SC medium; hydroxyurea (Sigma-Aldrich, H8627): 0.2M in YPD; MMS: methyl methanesulfonate (Sigma-Aldrich, 129925), 0.05% in YPD; benomyl (Sigma-Aldrich, 381586): 15 μg/mL in YPD; cycloheximide (Sigma-Aldrich, 01810): 10 μg/mL in YPD liquid medium for 2 h followed by plating to YPD; H_2O_2 (Millipore, 88597): 1 mM in YPD liquid medium for 2 h followed by plating to YPD. For chromoduction experiments, SC–Lys–Arg or SC–Leu–Arg plates were used with cycloheximide (10 μg/mL) and canavanine (12 μg/mL) added. For chromosome destabilization, strains were grown in YPD with 2% galactose and 1% raffinose added. Sporulation medium was prepared using a 50x base consisting of 50 g potassium acetate and 0.25 g zinc acetate dihydrate in 100 mL H2O. Final 1x sporulation media was prepared from 2 mL of 50x sporulation medium base plus 300 μL of 10% yeast extract, 200 μM uracil, 2 mM leucine 300 μM histidine, and H_2O to 100 mL.

Minichunk assembly

Minichunks were originally assembled according to the following process, similar to the one previously described for *synIII*:[5] First, approximately 70-mer oligonucleotides with 20-mer overlaps were designed using GeneDesign software[40] and assembled by members of the Build A Genome class at Johns Hopkins University using polymerase cycling assembly (PCA) to produce 750 bp building blocks. Building blocks were verified by sequencing. Overlapping building blocks with approximately 40 bp overlaps were then assembled into 2-4 kb minichunks by direct homologous recombination in yeast. Minichunks were recovered from yeast into *E. coli*, and the recovered minichunk plasmids were verified by sequencing.

Later minichunks were ordered directly from DNA synthesis vendors with flanking *Not*I or *Bbs*I sites, verified by sequencing, excised from the vectors in which they were built via restriction digestion or, for those containing internal *Not*I or *Bbs*I sites, amplified by PCR, and integrated directly into the *synIX* strain or used for megachunk assembly.

Megachunk assembly and verification

Unlike the subsequent chromosomes, *synIX* was initially designed in separate "left and right" halves, which were subsequently merged. During the design process, *synIXL* was originally divided into megachunks A-F and V-Z. Following the integration of megachunks A-F as described in the "Minichunk integration by SwAP-In" section, the minichunks comprising megachunks V-Z in the original *synIX* design were reapportioned into three new megachunks, designated G, H, and I. Each megachunk plasmid was designed with flanking *Not*I sites for eventual excision of the assembled megachunk, 13-16 minichunks, a terminal selectable marker (*LEU2* or *URA3*, for use with SwAP-In), and homology arms between the first and last minichunks and the plasmid backbone. Overlaps between segments ranged from approximately 100-800 bp. Minichunks were released from their backbone plasmids or amplified by PCR, and were co-transformed with linkers and megachunk backbone plasmid into wild-type yeast (BY4741). Following plasmid assembly in yeast by homologous recombination and two days of growth on appropriate selective medium (SC–Leu or SC–Ura) at 30°C, single colonies were isolated and assessed by PCR to detect the presence or absence of each desired assembly junction. Colonies containing all desired junctions were recovered from yeast by phenol extraction and isopropanol precipitation, and subsequently electroporated into EPI300 *E. coli* cells (Lucigen, EC300150). Megachunk plasmids were extracted from *E. coli* using the PureLink™ HiPure Plasmid Midiprep Kit (Invitrogen, K2100-15).

To verify the sequences of the recovered megachunk plasmids, DNA sequencing libraries were prepared using 300 ng of plasmid DNA as input for the NEBNext Ultra II FS DNA Library Kit (NEB, E7805). DNA libraries were sequenced via Illumina NextSeq 500 using 36 bp pair-end reads. Following sequencing, reads were first processed using Trimmomatic v0.39[42] and FastQC v0.11.4[43] aligned to an appropriate reference sequence using bowtie2 v2.2.9,[44] and visualized using IGV v2.7.2.[41]

Minichunk integration by SwAP-In

Minichunks were released from their backbones by restriction enzyme digestion, and the minichunks corresponding to one megachunk in the *synIX* design sequence (approximately 11-16 minichunks) were cotransformed into the partially completed *synIX* strain. Integration began at the left telomere of chromosome *IX* and proceeded in a stepwise fashion towards the centromere. At each step, the rightmost minichunk integrated contained either a *URA3* or a *LEU2* auxotrophic marker. These markers were alternated at each step according to the principles of Switching Auxotrophies Progressively for Integration (SwAP-In),[2,6] and colonies containing the new marker and lacking the previous strain's marker were identified by replica plating. Strains were assessed by PCRTag analysis after each round of integration.

Megachunk integration by SwAP-In

Sequence-verified megachunks were released from their assembly backbones via *Not*I digestion. Approximately 1 μg of digest product was transformed into the semisynthetic *synIX* strain, and cells were grown for two days at 30°C on appropriate SC dropout plates to select for the desired integration product. As with minichunk integration by SwAP-In, alternating *LEU2* and *URA3* auxotrophic markers were used each round, enabling selection of colonies containing the desired new integration marker and a lack of the previous round's integration marker, as determined by replica plating. Colonies were assessed by PCRTag analysis, and colonies containing the desired

PCRTags of interest were used for subsequent megachunk integration rounds. After integration of all three megachunks introduced by this method, yeast strain sequences were verified by whole genome sequencing, as described in the "Whole genome sequencing" section. To remove the *URA3* marker introduced during megachunk I integration, a PCR product with homology arms flanking *URA3* was transformed into the *synIX* strain, and colonies lacking the *URA3* marker were obtained following growth on 5-FOA medium.

PCRTag analysis

Cells from a single yeast colony were scraped from a plate using a pipette tip and resuspended in 30 μL of 20 mM sodium hydroxide in a 96-well PCR plate. The PCR plate was sealed and placed in a thermal cycler using the following boiling cycle: 3 cycles of 98°C for 3 m and 4°C for 1 m. 1 μL of boiled product and 0.5 μM each primer were used in a 5 μL reaction using the GoTaq Green PCR system (Promega, M7123). An acoustic liquid handler (Labcyte, Echo 550) transferred primers and DNA template. Samples were run through the following protocol in a 384-well thermal cycler: 95°C for 5 m, 30 cycles of 95°C for 30 s, 55°C for 90 s, and 72°C for 60 s, and a final extension step of 72°C for 7 m. Samples were visualized following electrophoresis on a 1% agarose in 1X Tris-Taurine-EDTA gel containing ethidium bromide using the ChemiDoc XRS+ System (Bio-Rad).

Growth assays

A single yeast colony for each strain was inoculated into 5 mL YPD and incubated at 30°C overnight with rotation. For assays monitoring strain growth across multiple passages, overnight cultures were diluted 1:1000 in YPD and incubated at 30°C overnight with rotation until reaching the desired passage number. Overnight yeast culture was diluted to A_{600}=0.15 into 6 mL of fresh YPD liquid medium and grown at 30°C with rotation until A_{600} reached 0.5-0.6. Cultures were serially diluted in tenfold increments in water, with a target OD of approximately 0.1 in 100 μL total volume for the first row of the wild-type control strain used to determine the starting culture volume in water for each sample. 5 μL (YPD and YPG plates) or 10 μL (SC plates) of each dilution was spotted to each plate. Plates were grown at appropriate temperatures (room temperature of approximately 22°C on YPD, 30°C on YPD, YPG, and SC, and 37°C on YPD and YPG) and photographed daily. For additional media types (**Figures S18 and S19**), plates were prepared as described in the "Yeast media" section. Strains were serially diluted in tenfold increments of water as described above, and 5 μL of each dilution was spotted to each plate. Plates were grown at 30°C and photographed daily.

Plate reader growth assays in liquid culture

Three single yeast colonies per strain of interest were resuspended in 1 mL YPD in a 2 mL deep well plate and incubated for 24 h at 30°C with shaking at 800 rpm. Saturated cultures were diluted 1:100 in 200 μL YPD in a glass bottom 96-well plate with lid (Greiner Bio-One, 655892) and loaded into a Cytation 5 cell imaging multimode reader (Agilent). The following program was run using the Cytation 5 Gen5 software: 32 h at 37°C with continuous shaking, with A_{600} measured every 10 m. Data analysis and visualization were conducted using Microsoft Excel and GraphPad Prism 9.

Genome editing using CRISPR-Cas9

A two-plasmid system with one guide RNA (gRNA) plasmid and one Cas9 plasmid was used for most editing.[52] The Cas9 coding sequence was assembled together with a *TEF1* promoter and *CYC1* terminator in a pRS415 plasmid backbone (with *LEU2* marker). This plasmid was pre-transformed into yeast strains prior to the introduction of the gRNA plasmid and donor DNA. Guide RNA target sequences were selected by identifying 20 bp upstream of the desired protospacer adjacent motif (PAM) sequence (NGG). gRNAs were cloned into a 2-micron plasmid (pRS426, with *URA3* marker) under the control of a *SNR52* promoter using Gibson assembly. A modified version of the gRNA plasmid was used for editing two loci simultaneously. In this case, a second gRNA was cloned into the plasmid under control of a *RPR1* promoter and *RPR1* terminator. gRNA sequences were confirmed by Sanger sequencing (Genewiz). To edit the *synIX* strain, approximately 50 ng of gRNA plasmid and 200-300 fmol (for minichunk patch replacement) or 1 pmol (for point mutation fixing) of donor DNA were transformed into yeast cells containing the Cas9 plasmid. Cells were grown on dropout medium to select for the presence of both the Cas9 and gRNA plasmids, and editing was confirmed using either PCRTag analysis or PCR followed by Sanger sequencing (Genewiz).

Sporulation and tetrad dissection experiments for bug mapping

The *synIX* strain yLHM1192 was crossed to a wild-type yeast strain (BY4742 with a *URA3-pGAL-CEN9* cassette integrated near the centromere, also known as yLHM0539) to generate a heterozygous diploid (yLHM1233) with one copy of wild-type chromosome *IX* and one copy of *synIX*. To prepare strains for sporulation, a single colony of each strain was inoculated into 5 mL YPD and incubated at 30°C overnight with rotation. Overnight cultures were diluted to an OD of ~1 in YPD and grown to an OD of ~4, washed five times with water, and resuspended in 2 mL of 1X sporulation medium. Strains were incubated at room temperature for 7-10 days with rotation, and monitored for the presence of tetrads. For tetrad dissection, 100 μL of these resuspended yeast cells in sporulation medium were washed and incubated with 25 μL of 0.5 mg/mL zymolyase in 1M sorbitol for 8 m. 200 μL of 1M sorbitol was added to the cells, and 10 μL of the resulting mixture was added to a YPD plate. Tetrads were separated and picked using a dissection microscope (Singer Instruments). Spores were grown for 2-3 days on YPD until visible colonies emerged. These strains were used for growth assays as described in the "Growth assays" section to classify each spore as healthy (similar fitness to the wild-type parent) or sick (similar fitness to the *synIX* parent). Strains from eighteen four-spore tetrads (72 strains) were prepared for whole genome sequencing, as described in the "Whole genome sequencing" section below.

Plasmid cloning and transformation for *synIX* bug mapping

Wild-type genes of interest plus approximately 500 bp of upstream flanking sequence and 200 bp of downstream flanking sequence were amplified from BY4741 by PCR. Genes were cloned into plasmid pRS413 linearized with *Afe*I by Gibson assembly and transformed into TOP10 cells. Colonies were grown up in 2 mL LB + 75 μg/mL carbenicillin and miniprepped using the Zyppy Plasmid Miniprep Kit (Zymo Research, D4037). Plasmid insert sequences were verified by Sanger sequencing. Plasmids were subsequently transformed into the *synIX* strain and grown for two days on SC–His plates. Yeast colonies containing each plasmid of interest were isolated, grown in SC–

His liquid medium, and used for growth assays (as described in the "Growth assays" section) to assess their relative fitness compared to the starting *synIX* strain.

Selective destabilization and loss of one copy of *synIX* from disomic strain

A cassette containing a galactose-inducible centromere and a *URA3* marker (*URA3-pGAL-CEN9*) with homology arms matching *synIX* was amplified by PCR and transformed into the *synIX* strain. After two days of growth at 30°C on SC–Ura plates, single colonies were purified and assessed by junction PCR for the insertion of the *URA3-pGAL-CEN9* fragment. Strains were then grown in YEP + 2% galactose + 1% raffinose for two days and diluted to 5-FOA plates to obtain single colonies lacking *URA3*. Strains were single-colony purified and prepared for whole genome sequencing to assess chromosome copy number.

Whole genome sequencing

A single yeast colony was inoculated into 5 mL of YPD liquid medium at 30°C overnight with rotation. Overnight cultured yeast cells were harvested by centrifugation at 3000 x g for 3 m, and yeast genomic DNA was extracted using the Fungi/Yeast Genomic DNA Isolation Kit (Norgen, 27300). Genomic DNA concentration was determined using the Qubit dsDNA HS Assay Kit (Thermo Fisher Scientific, Q32854). DNA sequencing libraries were prepared using 300 ng of yeast genomic DNA as input for the NEBNext Ultra II FS DNA Library Kit (NEB, E7805). DNA libraries were sequenced via Illumina NextSeq 500 using either 75 bp or 36 bp pair-end reads. Following sequencing, reads were first processed using Trimmomatic v0.39[42] and FastQC v0.11.4,[43] aligned to an appropriate reference genome using bowtie2 v2.2.9,[44] and visualized using IGV v2.7.2.[41] Chromosome coverage plots were prepared in Rstudio version 1.3.1093 using the ggplot2 v3.3.5 package.[45]

Southern blot analysis

A single yeast colony was inoculated into 10 mL of YPD medium at 30°C overnight with rotation. Overnight cultured yeast cells were harvested by centrifugation at 3000 x g for 3 m, and yeast genomic DNA was extracted using the MasterPure™ Yeast DNA Purification Kit (Lucigen, MPY80200) according to the manufacturer's instructions, with an RNase A treatment step. DNA was quantified using the Qubit dsDNA BR Assay Kit (Thermo Fisher Scientific, Q32850). 2 μg of DNA were digested with *Xho*I at 37°C overnight. Digests were electrophoresed on a 1% Tris-Borate-EDTA gel in 0.5X Tris-Borate-EDTA running buffer for 10 h at 50V. Following electrophoresis, the gel was washed in depurination solution (0.25 M HCl) for 15 m, denaturation solution (0.5 M NaOH, 1.5 M NaCl) for 60 m, and neutralization solution (0.5 M Tris, 1.5 M NaCl, pH 7.5) for 30 m. Chromosomes were transferred by capillarity to a nylon membrane (Pall Corporation, 60207) using 10X SSC buffer (20X SSC: 1.5 M NaCl, 0.3 M sodium citrate, pH 7) for 18 h. After transfer, the membrane was washed in 2X SSC buffer for 5 m and baked at 80°C for 30 m. Prehybridization was performed for 60 m in ULTRAhyb™ Ultrasensitive Hybridization Buffer (Invitrogen, AM8669) at 55°C with rotation. For hybridization, probes were prepared by labeling a ~360 bp PCR fragment of universal telomere cap sequence from plasmid pJS160 using the PCR DIG Probe Synthesis Kit (Roche, 11636090910) with oligos 5'-GCTATACGAAGTTATTAGGGTAGTGTG-3' and 5'- CTGCAGGTCGACTCTAGAGGATC-3', according to the manufacturer's instructions. The following thermocycler conditions were used: 1 cycle of 95°C for 2 m, 30 cycles of 95°C for 30 s, 60°C for 30 s, and 72°C for 40 s, and a final elongation step of 72°C for 7 m. Probes were purified using Zymo-Spin I Columns (Zymo

Research, C1003) and denatured at 95°C for 5 m. Hybridization was performed at 55°C overnight with rotation in 10 mL ULTRAhyb™ Ultrasensitive Hybridization Buffer (Invitrogen, AM8669) using 500 ng of probe per experiment. The blot was washed twice with 2X SSPE buffer (20X SSPE buffer: 0.02 M EDTA and 2.98 M NaCl in 0.2 M phosphate buffer, pH 7.4; Sigma-Aldrich, S2015) for 5 m at room temperature, twice with 2X SSPE + 1% SDS for 30 m at 55°C, and twice with 0.1X SSPE for 15 m at 55°C. Blot was incubated overnight in 1:1 Intercept (TBS) Blocking Buffer (LI-COR Biosciences, 927-60001): 1X Tris-Buffered Saline (TBS) with 0.1% TWEEN 20 (Sigma-Aldrich, P1379) (1X TBST) and 1% SDS at room temperature. The next day, the membrane was washed with 1X TBST for 5 m and incubated for 1 hour at room temperature with rabbit anti-DIG antibody (working concentration 1:2500 in 1:1 Intercept (TBS) Blocking Buffer: 1X TBST; Invitrogen, 700772). The primary antibody solution was washed out three times with 1X TBST for 15 m at room temperature. The membrane was incubated in goat anti-rabbit IgG secondary solution (LI-COR Biosciences, 926-68071, used at 1:10,000 in 1:1 Intercept (TBS) Blocking Buffer (LI-COR Biosciences, 927-60001): 1X TBST with 1% SDS) for 1.5 h. The blot was washed three times with 1X TBST for 15 m at room temperature plus one time with 1X TBS for 30 m at room temperature. A LI-COR Odyssey Instrument was used to develop the blot images.[53]

RNA extraction, sequencing, and analysis for short read sequencing

A single yeast colony was inoculated into 5 mL of YPD liquid medium at 30°C overnight with rotation. Overnight yeast culture was diluted to A_{600}=0.15-0.2 into 6 mL of fresh YPD liquid medium and grown at 30°C or 37°C with rotation until A_{600} reached 0.8-1.0. Yeast cells were harvested from 4 mL of culture, and total RNA was extracted using the RNeasy Mini Kit (QIAGEN, 74106) according to the manufacturer's instructions. RNA was quantified using the Qubit BR RNA Assay Kit (Thermo Fisher Scientific, Q10210). 1 μg total RNA was used as input for the QIAseq Stranded Total RNA Library Kit (QIAGEN, 180745) plus QIAseq FastSelect -rRNA Yeast Kit (QIAGEN, 334217). RNA libraries were sequenced via Illumina NextSeq 500 using 75 bp paired-end reads. For applications requiring similar numbers of reads per sample, downsampling was performed using seqtk v1.3. Samples were first processed using Trimmomatic v0.39[42] and FastQC v0.11.4.[43] Processed reads were aligned to the S288C transcriptome and a custom *synIX* transcriptome (in which chromosome *IX* transcripts were replaced with their synthetic versions) using Kallisto v0.46.0[46] and STAR v2.5.2a.[47] STAR-aligned results were further processed using SAMtools v1.9[48] and BEDtools v2.26.0,[49] and visualized in IGV v2.7.2.[41] Kallisto pseudoalignment data was further processed in Rstudio version 1.3.1093 using the sleuth v0.30.0[50] and ggplot2 v3.3.5[45] packages. For volcano plots, we calculated effect scores (approximately log2 fold change values), tested results for significance using Wald's test, and corrected for multiple testing with the false discovery rate adjusted p-value using the Benjamini-Hochberg method. The following genes deleted from the *synIX* design were removed from the plots in **Figure 4D** and **Figure 4E**: YIL173W (VTH1), YIL171W (part of HTX12 pseudogene), YIL170W (part of HTX12 pseudogene), YIL169C (CSS1), YIL167W (SDL1, blocked reading frame), YIL082W, YIL060W, YIL059C, YIL058W, YILWTy3-1, YILCdelta3. The following dubious ORFs, retrotransposable elements, and subtelomeric genes were also removed: YBL100C, YGR296C-B, YHL050W-A, YHR219C-A, YIL020C-A, YJR029W, YLL066C, YML133W-B, YMR046C, YNL339W-B, YNL339C, YOR277C, YPL283W-B, YPR158W-B, YPR204C-A, YBLWdelta4, YCLWdelta3. Unfiltered versions of the volcano plots are depicted in **Figure S20**.

RNA extraction, sequencing, and analysis for nanopore direct RNA sequencing

Methods recently described by us were used to perform nanopore sequencing to analyze RNA isoforms.[54] Total RNA was extracted from 50 mL flash-frozen cell pellets grown to mid-log (OD_{600} ~0.65-0.85) using the MasterPure™ Yeast RNA Purification Kit (Lucigen) including a Dnase I treatment step. RNA (diluted 1:10) quality and concentration were measured by Agilent 2100 Bioanalyzer with the Agilent RNA 6000 Nano Kit and Qubit™ RNA High Sensitivity Kit (Thermo Fisher Scientific), respectively. Poly(A) mRNA was enriched from 50 μg total RNA on 132 μL Dynabeads oligo$(dT)_{25}$ beads. The Direct RNA Sequencing Kit (SQK-RNA002, Oxford Nanopore Technologies) was used to generate libraries from 500 ng poly(A) RNA. An optional reverse transcription was performed at 50°C for 50 m using SuperScript™ IV Reverse Transcriptase (Invitrogen) in between the ligation of the RTA and RMX adaptors. Following reverse transcription the RNA:cDNA was cleaned up with 1.8 volumes of Agencourt RNAClean XP beads and washed with 70% ethanol. Following RMX ligation only one volume of beads was used in the clean-up, and WSB (SQK-RNA002) was used in the wash steps. Direct RNA libraries (typically 150-200 ng) were loaded onto primed (EXP-FLP001) MinION flow cells (FLO-MIN106D, R9 version) in RRB buffer and run on the GridION with MinKNOW 5.2.2 for up to 72 h. Nanopore long reads were base-called, trimmed of adapter sequences, and filtered for quality, retaining only those with the best alignment scores for multi-mapping reads, as previously described.[54] For TSS distributions, long-reads that overlapped at least 75% of the annotated gene were used.

Construction of FLAG-tagged *EST3* strains

A DNA fragment containing a six-glycine linker plus a 3X FLAG tag (DYKDHDG-DYKDHDI-DYKDDDDK) was designed for integration at the 3' end of *EST3*, in-frame with the rest of the protein and inserted just before the *EST3* stop codon. The segment containing the tag was flanked by 70-100 bp homology arms matching the yeast genome sequence adjacent to the desired insertion site. Genome editing using CRISPR-Cas9 in yeast (as describe above) was used to cut the genome near the end of the *EST3* coding sequence and insert the tag of interest. Colony PCR and Sanger sequencing (Genewiz) were used to confirm in-frame insertion of the tag.

Immunoblot analysis

A single yeast colony was inoculated into 5 mL of YPD liquid medium at 37°C overnight with rotation. Overnight culture was diluted to A_{600}=0.15-0.2 into 50 mL of fresh YPD liquid medium and grown at 37°C with rotation until A_{600} reached 0.8-1.0. Yeast were harvested by centrifugation, and pellets were frozen overnight at -80C. Pellets were subsequently resuspended in 500 μL of lysis buffer (20 mM HEPES pH 7.4, 1% Triton™ X-100 (Sigma-Aldrich, X100), 2 mM $MgCl_2$, 500 μM NaCl, and 1X protease inhibitor (Roche)). Cell suspension was added to MP Biomedicals FastPrep Lysing Matrix C and subjected to the following shaking program at 4°C using a FastPrep-24 5G (MP Biomedicals): 7 cycles of 15 s shaking at 6.0 m/second + 30 s rest between cycles. Samples were centrifuged at 13000 x g for 10 m at 4°C, and 30 μL of supernatant was transferred to a new tube and mixed with 10 μL of 4X LDS loading buffer (Invitrogen, NP0007) (pre-immunoprecipitation sample). The remaining supernatant was transferred to pre-equilibrated FLAG M2 (Sigma F1804)-conjugated M-270 Dynabeads (Invitrogen, 14302D) for immunoprecipitation.[55] Samples with beads were incubated on ice for 60 m, washed 3 times with lysis buffer, and eluted at 70°C with shaking

at 700 rpm in 50 μL 1.1X LDS loading buffer (Invitrogen, NP0007) in lysis buffer for 10 m. 2-mercaptoethanol (1.43 M final) was added, and samples were heated to 95°C for 5 m and loaded onto an SDS-PAGE gel for immunoblotting. Mouse anti-FLAG M2 antibody (Sigma F1804, used at 1:5000) and rabbit [54] anti-histone H3 antibody (Abcam, 1791, used at 1:5000) were used for blotting proteins of interest overnight at 4°C. Goat anti-mouse IgG1 (LI-COR Biosciences, 926-32350, used at 1:20,000) and goat anti-rabbit IgG (LI-COR Biosciences, 926-68071, used at 1:20,000) were used for blotting FLAG and H3 primary antibodies, respectively, during a one-hour incubation at room temperature. A LI-COR Odyssey Instrument was used to develop the blot images.[53]

Pulsed-field gel electrophoresis

A single yeast colony was inoculated into 7 mL of YPD liquid medium and grown at 30°C for two days with rotation. Approximately 40 mg of yeast cells were harvested by centrifugation. To prepare plugs, 16 μL of zymolyase solution (25 mg/mL zymolyase 20T in 10 mM KH_2PO_2 pH 7.5) and 360 μL of 0.5% melted low melting point agarose (Bio-Rad, 1620137) in 100 mM EDTA pH 7.5 were added to the cell pellet and mixed by pipetting. 90 μL of this suspension was added per well of a BioRad plug mold, and the plugs were cooled for 30 m at 4°C. Solidified plugs were then transferred into 15 mL tubes containing 1 mL of digestion buffer (0.5 M EDTA, 10 mM Tris, pH 7.5), mixed by inversion, and incubated at 37°C with rotation overnight. The next day, 400 μL of proteinase K solution (5% sarcosyl and 5 mg/mL proteinase K in 0.5 M EDTA, pH 7.5) were added to the tube. Samples were incubated at 50°C for five h, and then washed once with H_2O and three times with TE (2 mM Tris, 1 mM EDTA, pH 8.0). Plugs were stored at 4°C until ready for gel loading. Half of one plug per sample was embedded per well of a gel consisting of 1% low melting point agarose in 0.5X Tris-Borate-EDTA buffer. Samples were separated in running buffer of 0.5X Tris-Borate-EDTA by clamped homogeneous electric field gel electrophoresis using the CHEF Mapper XA Pulsed-Field Electrophoresis System (Bio-Rad), as previously described.[56] The following program was used: auto-algorithm with size range of 200 kb to 2.5 Mb, temperature of 14°C, voltage of 6 V/cm, included angle of 120°. After electrophoresis, gels were stained using 5 μg/mL ethidium bromide in water for 30 m, destained in water for 30 m, and then imaged using the ChemiDoc XRS+ System (Bio-Rad).

Chromosome substitution and conditional centromere destabilization

For initial experiments, disomic *synIX* strain yLHM0387 was used as the donor and yWZ601 as the recipient for *kar1-1*-mediated chromoduction. For follow-up experiments, disomic strain yLHM0604 and monosomic strains yLHM0721, yLHM1591, and yLHM1601 were used as donors and yWZ602 as the recipient for *kar1-1*-mediated chromoduction. yWZ601 and yWZ602 were derived from DMy044[24] following deletion of *LYS12* from wild-type chromosome *IX* and insertion of a *URA3-pGAL* promoter cassette upstream of *CEN9*.[26] Strains were grown independently on YPD plates, and subsequently mated on YPD plates via replica plating. After 14 h of growth, these plates were replica plated to SC–Lys–Arg plates with 12 μg/mL canavanine and 10 μg/mL cycloheximide added. Plates were grown until individual colonies emerged; if a patched formed instead, patches were replica plated to the same selective medium and grown for additional time until individual colonies emerged. Single colonies were restreaked to fresh selective plates and analyzed by

PCRTagging, pulsed-field gel electrophoresis, and whole genome sequencing. To lose wild-type chromosome *IX*, strains were grown in YPD overnight, diluted 1:1000 in YEP + 2% galactose medium for 24 h, and plated on 5-FOA medium to select for strains that had lost wild-type chromosome *IX*. Single colonies were genotyped by PCRTag analysis and further characterized by pulsed-field gel electrophoresis and whole genome sequencing. For chromosome substitution to move *synIX* from yLHM1601 to recipient strain yLHM2231 (derived from BY4742), a LEU2 marker was integrated into *synIX* near the end of megachunk H, in minichunk 101, generating strain yLHM1754. The same protocol as listed above was followed using donor strain yLHM1754 and recipient strain yLHM2231, except after mating and 14 h of growth, plates were replica plated to SC–Leu–Arg (rather than SC–Lys–Arg) plates with 12 μg/mL canavanine and 10 μg/mL cycloheximide added.

Acknowledgments

We thank Meghan O'Keefe for collecting the BAG student authors' information. We thank the NSF for grants MCB-1026068, MCB-1443299, MCB-1616111 and MCB-1921641 to JDB and MCB-1445545 to JSB for supporting this work.

Competing Interests

Jef Boeke is a Founder and Director of CDI Labs, Inc., a Founder of and consultant to Neochromosome, Inc, a Founder, SAB member of and consultant to ReOpen Diagnostics, LLC and serves or served on the Scientific Advisory Board of the following: Logomix, Inc., Sangamo, Inc., Modern Meadow, Inc., Rome Therapeutics, Inc., Sample6, Inc., Tessera Therapeutics, Inc. and the Wyss Institute. Joel Bader is a founder of Neochromosome, Inc., consultant to Opentrons Labworks, Inc. and advisor to Reflexion Pharmaceuticals, Inc.

Author contributions

J.D.B., S.C., and W.Z. conceptualized the study. W.Z., S.C., L.H.M., and J.D.B. designed the experiments. J.D.B. and J.S.B. designed *synIX*. The Build A Genome class members constructed building blocks. J.S., E.C., H.M., and K.Z led Build A Genome class research. V.S., N.A., and S.R. constructed minichunks and incorporated them for megachunks A to F. L.H.M. designed, constructed, and delivered megachunks G through I and performed error correction, bug mapping, bug correction, and functional studies of *synIX*. L.H.M. and W.Z. developed and evaluated chromosome substitution method. L.H.M., A.L.H., J.C., V.F., E.L., and G.S. performed sequencing and data analyses. L.H.M., W.Z., and J.D.B. wrote the manuscript. L.A.M., H.J., J.L., M.S.T., and W.R.B. provided advice. S.C., J.D.B., J.S.B., and L.M.S. provided lab supervision. All authors reviewed and edited the manuscript.

References

1. Dymond, J., and Boeke, J. (2012). The Saccharomyces cerevisiae SCRaMbLE system and genome minimization. Bioeng Bugs *3*, 168-171. 10.4161/bbug.19543.

2. Richardson, S.M., Mitchell, L.A., Stracquadanio, G., Yang, K., Dymond, J.S., DiCarlo, J.E., Lee, D., Huang, C.L., Chandrasegaran, S., Cai, Y., et al. (2017). Design of a synthetic yeast genome. Science *355*, 1040-1044. 10.1126/science.aaf4557.

3. Shen, M.J., Wu, Y., Yang, K., Li, Y., Xu, H., Zhang, H., Li, B.Z., Li, X., Xiao, W.H., Zhou, X., et al. (2018). Heterozygous diploid and interspecies SCRaMbLEing. Nat Commun *9*, 1934. 10.1038/s41467-018-04157-0.

4. Shen, Y., Stracquadanio, G., Wang, Y., Yang, K., Mitchell, L.A., Xue, Y., Cai, Y., Chen, T., Dymond, J.S., Kang, K., et al. (2016). SCRaMbLE generates designed combinatorial stochastic diversity in synthetic chromosomes. Genome Res *26*, 36-49. 10.1101/gr.193433.115.

5. Annaluru, N., Muller, H., Mitchell, L.A., Ramalingam, S., Stracquadanio, G., Richardson, S.M., Dymond, J.S., Kuang, Z., Scheifele, L.Z., Cooper, E.M., et al. (2014). Total synthesis of a functional designer eukaryotic chromosome. Science *344*, 55-58. 10.1126/science.1249252.

6. Dymond, J.S., Richardson, S.M., Coombes, C.E., Babatz, T., Muller, H., Annaluru, N., Blake, W.J., Schwerzmann, J.W., Dai, J., Lindstrom, D.L., et al. (2011). Synthetic chromosome arms function in yeast and generate phenotypic diversity by design. Nature *477*, 471-476. 10.1038/nature10403.

7. Mitchell, L.A., Wang, A., Stracquadanio, G., Kuang, Z., Wang, X., Yang, K., Richardson, S., Martin, J.A., Zhao, Y., Walker, R., et al. (2017). Synthesis, debugging, and effects of synthetic chromosome consolidation: synVI and beyond. Science *355*. 10.1126/science.aaf4831.

8. Shen, Y., Wang, Y., Chen, T., Gao, F., Gong, J., Abramczyk, D., Walker, R., Zhao, H., Chen, S., Liu, W., et al. (2017). Deep functional analysis of synII, a 770-kilobase synthetic yeast chromosome. Science *355*. 10.1126/science.aaf4791.

9. Wu, Y., Li, B.Z., Zhao, M., Mitchell, L.A., Xie, Z.X., Lin, Q.H., Wang, X., Xiao, W.H., Wang, Y., Zhou, X., et al. (2017). Bug mapping and fitness testing of chemically synthesized chromosome X. Science *355*. 10.1126/science.aaf4706.

10. Xie, Z.X., Li, B.Z., Mitchell, L.A., Wu, Y., Qi, X., Jin, Z., Jia, B., Wang, X., Zeng, B.X., Liu, H.M., et al. (2017). "Perfect" designer chromosome V and behavior of a ring derivative. Science *355*. 10.1126/science.aaf4704.

11. Zhang, W., Zhao, G., Luo, Z., Lin, Y., Wang, L., Guo, Y., Wang, A., Jiang, S., Jiang, Q., Gong, J., et al. (2017). Engineering the ribosomal DNA in a megabase synthetic chromosome. Science *355*. 10.1126/science.aaf3981.

12. Zhang, W., Lazar-Stefanita, L., Yamashita, H., Shen, M.J., Mitchell, L.A., Kurasawa, H., Haase, M.A.B., Sun, X., Jiang, Q., Lauer, S.L., et al. (2022). Manipulating the 3D

organization of the largest synthetic yeast chromosome. 2022.2004.2009.487066. 10.1101/2022.04.09.487066 %J bioRxiv.

13. Blount, B.A., Lu, X., Driessen, M.R.M., Jovicevic, D., Sanchez, M.I., Ciurkot, K., Zhao, Y., Lauer, S., McKiernan, R.M., Gowers, G.-O.F., et al. (2022). Synthetic yeast chromosome XI design enables extrachromosomal circular DNA formation on demand. 2022.2007.2015.500197. 10.1101/2022.07.15.500197 %J bioRxiv.

14. Williams, T.C., Kroukamp, H., Xu, X., Wightman, E.L.I., Llorente, B., Borneman, A.R., Carpenter, A.C., Van Wyk, N., Espinosa, M.I., Daniel, E.L., et al. (2022). Laboratory evolution and polyploid SCRaMbLE reveal genomic plasticity to synthetic chromosome defects and rearrangements. 2022.2007.2022.501046. 10.1101/2022.07.22.501046 %J bioRxiv.

15. Schindler, D., Walker, R.S.K., Jiang, S., Brooks, A.N., Wang, Y., Müller, C.A., Cockram, C., Luo, Y., García, A., Schraivogel, D., et al. (2022). Design, Construction, and Functional Characterization of a tRNA Neochromosome in Yeast. 2022.2010.2003.510608. 10.1101/2022.10.03.510608 %J bioRxiv.

16. Shen, Y., Gao, F., Wang, Y., Wang, Y., Zheng, J., Gong, J., Zhang, J., Luo, Z., Schindler, D., Deng, Y., et al. (2022). Dissecting aneuploidy phenotypes by constructing Sc2.0 chromosome VII and SCRaMbLEing synthetic disomic yeast. 2022.2009.2001.506252. 10.1101/2022.09.01.506252 %J bioRxiv.

17. Luo, J., Mercy, G., Vale-Silva, L.A., Sun, X., Agmon, N., Zhang, W., Yang, K., Stracquadanio, G., Thierry, A., Ahn, J.Y., et al. (2018). Synthetic chromosome fusion: effects on genome structure and function. 381137. 10.1101/381137 %J bioRxiv.

18. Lendvay, T.S., Morris, D.K., Sah, J., Balasubramanian, B., and Lundblad, V. (1996). Senescence mutants of Saccharomyces cerevisiae with a defect in telomere replication identify three additional EST genes. Genetics *144*, 1399-1412. 10.1093/genetics/144.4.1399.

19. Morris, D.K., and Lundblad, V. (1997). Programmed translational frameshifting in a gene required for yeast telomere replication. Curr Biol *7*, 969-976. 10.1016/s0960-9822(06)00416-7.

20. Hughes, T.R., Evans, S.K., Weilbaecher, R.G., and Lundblad, V. (2000). The Est3 protein is a subunit of yeast telomerase. Curr Biol *10*, 809-812. 10.1016/s0960-9822(00)00562-5.

21. Zhao, Y., Coelho, C., Hughes, A.L., Lazar-Stefanita, L., Yang, S., Brooks, A.N., Walker, R.S.K., Zhang, W., Lauer, S., Hernandez, C., et al. (2022). Debugging and consolidating multiple synthetic chromosomes reveals combinatorial genetic interactions. 2022.2004.2011.486913. 10.1101/2022.04.11.486913 %J bioRxiv.

22. Conde, J., and Fink, G.R. (1976). A mutant of Saccharomyces cerevisiae defective for nuclear fusion. Proceedings of the National Academy of Sciences of the United States of America *73*, 3651-3655. 10.1073/pnas.73.10.3651.

23. Dutcher, S.K. (1981). Internuclear transfer of genetic information in kar1-1/KAR1 heterokaryons in Saccharomyces cerevisiae. Mol Cell Biol *1*, 245-253. 10.1128/mcb.1.3.245-253.1981.

24. Ji, H., Moore, D.P., Blomberg, M.A., Braiterman, L.T., Voytas, D.F., Natsoulis, G., and Boeke, J.D. (1993). Hotspots for unselected Ty1 transposition events on yeast chromosome III are near tRNA genes and LTR sequences. Cell *73*, 1007-1018. 10.1016/0092-8674(93)90278-x.

25. Guo, Z., Yin, H., Ma, L., Li, J., Ma, J., Wu, Y., and Yuan, Y. (2022). Direct Transfer and Consolidation of Synthetic Yeast Chromosomes by Abortive Mating and Chromosome Elimination. ACS Synth Biol. 10.1021/acssynbio.2c00174.

26. Reid, R.J., Sunjevaric, I., Voth, W.P., Ciccone, S., Du, W., Olsen, A.E., Stillman, D.J., and Rothstein, R. (2008). Chromosome-scale genetic mapping using a set of 16 conditionally stable Saccharomyces cerevisiae chromosomes. Genetics *180*, 1799-1808. 10.1534/genetics.108.087999.

27. Johnson, D.R., Knoll, L.J., Levin, D.E., and Gordon, J.I. (1994). Saccharomyces cerevisiae contains four fatty acid activation (FAA) genes: an assessment of their role in regulating protein N-myristoylation and cellular lipid metabolism. J Cell Biol *127*, 751-762. 10.1083/jcb.127.3.751.

28. Knoll, L.J., Johnson, D.R., and Gordon, J.I. (1994). Biochemical studies of three Saccharomyces cerevisiae acyl-CoA synthetases, Faa1p, Faa2p, and Faa3p. J Biol Chem *269*, 16348-16356.

29. Yoshikawa, K., Tanaka, T., Ida, Y., Furusawa, C., Hirasawa, T., and Shimizu, H. (2011). Comprehensive phenotypic analysis of single-gene deletion and overexpression strains of Saccharomyces cerevisiae. Yeast *28*, 349-361. 10.1002/yea.1843.

30. Devine, S.E., and Boeke, J.D. (1996). Integration of the yeast retrotransposon Ty1 is targeted to regions upstream of genes transcribed by RNA polymerase III. Genes Dev *10*, 620-633. 10.1101/gad.10.5.620.

31. Geiduschek, E.P., and Tocchini-Valentini, G.P. (1988). Transcription by RNA polymerase III. Annu Rev Biochem *57*, 873-914. 10.1146/annurev.bi.57.070188.004301.

32. Newman, A.J., Ogden, R.C., and Abelson, J. (1983). tRNA gene transcription in yeast: effects of specified base substitutions in the intragenic promoter. Cell *35*, 117-125. 10.1016/0092-8674(83)90214-3.

33. Hull, M.W., Erickson, J., Johnston, M., and Engelke, D.R. (1994). tRNA genes as transcriptional repressor elements. Mol Cell Biol *14*, 1266-1277. 10.1128/mcb.14.2.1266-1277.1994.

34. Fourel, G., Revardel, E., Koering, C.E., and Gilson, E. (1999). Cohabitation of insulators and silencing elements in yeast subtelomeric regions. EMBO J *18*, 2522-2537. 10.1093/emboj/18.9.2522.

35. Bolton, E.C., and Boeke, J.D. (2003). Transcriptional interactions between yeast tRNA genes, flanking genes and Ty elements: a genomic point of view. Genome Res *13*, 254-263. 10.1101/gr.612203.

36. Donze, D. (2012). Extra-transcriptional functions of RNA Polymerase III complexes: TFIIIC as a potential global chromatin bookmark. Gene *493*, 169-175. 10.1016/j.gene.2011.09.018.

37. Peter, J., De Chiara, M., Friedrich, A., Yue, J.X., Pflieger, D., Bergstrom, A., Sigwalt, A., Barre, B., Freel, K., Llored, A., et al. (2018). Genome evolution across 1,011 Saccharomyces cerevisiae isolates. Nature *556*, 339-344. 10.1038/s41586-018-0030-5.

38. Liti, G., Carter, D.M., Moses, A.M., Warringer, J., Parts, L., James, S.A., Davey, R.P., Roberts, I.N., Burt, A., Koufopanou, V., et al. (2009). Population genomics of domestic and wild yeasts. Nature *458*, 337-341. 10.1038/nature07743.

39. Strope, P.K., Skelly, D.A., Kozmin, S.G., Mahadevan, G., Stone, E.A., Magwene, P.M., Dietrich, F.S., and McCusker, J.H. (2015). The 100-genomes strains, an S. cerevisiae resource that illuminates its natural phenotypic and genotypic variation and emergence as an opportunistic pathogen. Genome Res *25*, 762-774. 10.1101/gr.185538.114.

40. Richardson, S.M., Wheelan, S.J., Yarrington, R.M., and Boeke, J.D. (2006). GeneDesign: rapid, automated design of multikilobase synthetic genes. Genome Res *16*, 550-556. 10.1101/gr.4431306.

41. Robinson, J.T., Thorvaldsdottir, H., Winckler, W., Guttman, M., Lander, E.S., Getz, G., and Mesirov, J.P. (2011). Integrative genomics viewer. Nat Biotechnol *29*, 24-26. 10.1038/nbt.1754.

42. Bolger, A.M., Lohse, M., and Usadel, B. (2014). Trimmomatic: a flexible trimmer for Illumina sequence data. Bioinformatics *30*, 2114-2120. 10.1093/bioinformatics/btu170.

43. Andrews, S. (2010). FastQC: a quality control tool for high throughput sequence data. http://www.bioinformatics.babraham.ac.uk/projects/fastqc/.

44. Langmead, B., and Salzberg, S.L. (2012). Fast gapped-read alignment with Bowtie 2. Nat Methods *9*, 357-359. 10.1038/nmeth.1923.

45. Wickham, H. (2016). ggplot2: Elegant Graphics for Data Analysis (Springer-Verlag New York).

46. Bray, N.L., Pimentel, H., Melsted, P., and Pachter, L. (2016). Near-optimal probabilistic RNA-seq quantification. Nat Biotechnol *34*, 525-527. 10.1038/nbt.3519.

47. Dobin, A., Davis, C.A., Schlesinger, F., Drenkow, J., Zaleski, C., Jha, S., Batut, P., Chaisson, M., and Gingeras, T.R. (2013). STAR: ultrafast universal RNA-seq aligner. Bioinformatics *29*, 15-21. 10.1093/bioinformatics/bts635.

48. Li, H., Handsaker, B., Wysoker, A., Fennell, T., Ruan, J., Homer, N., Marth, G., Abecasis, G., Durbin, R., and Genome Project Data Processing, S. (2009). The Sequence Alignment/Map format and SAMtools. Bioinformatics *25*, 2078-2079. 10.1093/bioinformatics/btp352.

49. Quinlan, A.R., and Hall, I.M. (2010). BEDTools: a flexible suite of utilities for comparing genomic features. Bioinformatics *26*, 841-842. 10.1093/bioinformatics/btq033.

50. Pimentel, H., Bray, N.L., Puente, S., Melsted, P., and Pachter, L. (2017). Differential analysis of RNA-seq incorporating quantification uncertainty. Nat Methods *14*, 687-690. 10.1038/nmeth.4324.

51. Brachmann, C.B., Davies, A., Cost, G.J., Caputo, E., Li, J., Hieter, P., and Boeke, J.D. (1998). Designer deletion strains derived from Saccharomyces cerevisiae S288C: a useful set of strains and plasmids for PCR-mediated gene disruption and other applications. Yeast *14*, 115-132. 10.1002/(SICI)1097-0061(19980130)14:2<115::AID-YEA204>3.0.CO;2-2.

52. DiCarlo, J.E., Norville, J.E., Mali, P., Rios, X., Aach, J., and Church, G.M. (2013). Genome engineering in Saccharomyces cerevisiae using CRISPR-Cas systems. Nucleic acids research *41*, 4336-4343. 10.1093/nar/gkt135.

53. Litovchick, L. (2020). Immunoblotting. Cold Spring Harb Protoc *2020*, 098392. 10.1101/pdb.top098392.

54. Brooks, A.N., Hughes, A.L., Clauder-Munster, S., Mitchell, L.A., Boeke, J.D., and Steinmetz, L.M. (2022). Transcriptional neighborhoods regulate transcript isoform lengths and expression levels. Science *375*, 1000-1005. 10.1126/science.abg0162.

55. Domanski, M., Molloy, K., Jiang, H., Chait, B.T., Rout, M.P., Jensen, T.H., and LaCava, J. (2012). Improved methodology for the affinity isolation of human protein complexes expressed at near endogenous levels. Biotechniques *0*, 1-6. 10.2144/000113864.

56. Luo, J., Sun, X., Cormack, B.P., and Boeke, J.D. (2018). Karyotype engineering by chromosome fusion leads to reproductive isolation in yeast. Nature *560*, 392-396. 10.1038/s41586-018-0374-x.